Trends in Food Science & Technology 124 (2022) 167–181

Contents lists available at ScienceDirect

Trends in Food Science & Technology

journal homepage: www.elsevier.com/locate/tifs

# Photodynamic inactivation in food systems: A review of its application, mechanisms, and future perspective

Lina Sheng [a,b], Xiran Li [b], Luxin Wang [b,*]

[a] State Key Laboratory of Food Science and Technology, School of Food Science and Technology, School of Food Science Synergetic Innovation Center of Food Safety and Nutrition, Jiangnan University, Wuxi, Jiangsu 214122, China
[b] Department of Food Science and Technology, University of California Davis, Davis, CA, 95616, United States

ARTICLE INFO

*Keywords:*
Photodynamic inactivation
Reactive oxygen species
Food
Mechanism
Resistance

ABSTRACT

*Background:* Foodborne illnesses caused by pathogenic microorganisms, food loss and waste caused by spoilage microorganisms, and the occurrence of antibiotic-resistant bacteria are of the greatest public concerns. Photodynamic inactivation (PDI) is a promising technology for mitigating the above challenges. Given the rapid advances in PDI and its increasing popularity in food decontamination, a comprehensive and updated review is needed to summarize the antimicrobial mechanisms of PDI against food-related microorganisms.

*Scope and approach:* This review discusses the principle behind PDI, its application in food decontamination and preservation, antimicrobial mechanisms, and impact on innate antimicrobial susceptibility of microorganisms. Special emphasis is given to the antimicrobial mechanisms of PDI, its biological targets, and impacts.

*Key findings and conclusions:* The chemistry behind PDI is the production of reactive oxygen species through the activation of endogenous or exogenous photosensitizers. PDI has proven its efficacy against pathogenic and spoilage bacteria, fungi, viruses, and spores in a variety of food and food contact surfaces. PDI's major antimicrobial mechanisms include disruption of cell structure and function, oxidation of macromolecules, inhibition of quorum sensing, disruption of biofilm, and attenuation of virulence factors. Development of PDI resistance is unlikely because of its multitargeted nature. Projects that investigate the long-term impacts of PDI treatments on food quality and safety as well as on human health, optimization of application parameters, and effective transformation of the laboratory-scale design to industrial-scale production are still needed for more advanced application of PDI in food systems.

## 1. Introduction

According to the Food and Agriculture Organization of the United Nations (FAO), food systems cover the whole range of actors and activities involved in the production, aggregation, processing, distribution, consumption, and disposal of food (FAO). A sustainable food system delivers food security and nutrition to all people in the world (FAO). Unfortunately, current food systems face several increasing and significant challenges. Among them, the increased incidence of food safety issues and high levels of food loss and waste are two key ones. As estimated by the World Health Organization (WHO) (2015), one in 10 people globally gets ill from contaminated food every year, resulting in an estimated 600 million illnesses, 420,000 deaths, and a loss of 33 million healthy life-years. The three main types of food safety contaminants are biological, chemical, and physical hazards (FDA). Foodborne pathogens including pathogenic bacteria, viruses, and parasites are the most frequent cause of foodborne illnesses and account for 230,000 annual deaths, 81.4% of which are caused by bacteria, followed by viruses (15.2%) and parasites (2.4%) (WHO, 2015). Food loss, according to the FAO, refers to the decrease in the quantity or quality of food along the food supply chain by food suppliers, while food waste occurs at the retail and consumer level (FAO). It is estimated that 14% of food produced globally is lost before reaching the retail stage (FAO). Food waste at the consumer level is critical, with 14–37% of animal products and 9–20% of fruits and vegetables wasted at the consumption stage worldwide (FAO).

Microorganisms play significant roles in food safety and food loss and waste. Of the 2953 foodborne outbreaks in the U.S. from 2009 to 2015 with a single confirmed etiology, norovirus (38%), *Salmonella* (30%), and Shiga toxin-producing *Escherichia coli* (STEC, 6%) were the

* Corresponding author.
*E-mail address:* lxwang@ucdavis.edu (L. Wang).

https://doi.org/10.1016/j.tifs.2022.04.001
Received 11 October 2021; Received in revised form 28 February 2022; Accepted 1 April 2022
Available online 14 April 2022

most common causes of outbreaks; and *Listeria*, *Salmonella*, and STEC were the most common causes of hospitalizations (82%) and deaths (82%) (Dewey-Mattia et al., 2018). Microbes have also been the most common cause of food spoilage. While food with high water content such as meat, milk, and seafood easily gets spoiled by bacteria, the spoilage of low-moisture food such as dried fruits and bakery goods is usually initiated by molds or yeasts (Doyle & Buchanan, 2013). In the past decade, the emergence and spread of antibiotic-resistant pathogenic and spoilage bacteria and fungicide-resistant fungi has become another significant challenge for the food system. For example, antibiotic-resistant or multidrug-resistant bacteria (e.g., *Salmonella*, *L. monocytogenes*, *Aeromonas hydrophila*) as well as antibiotic-resistant genes (ARGs) have been repeatedly detected in fish and fish products (Sheng & Wang, 2021).

In the last decade, photodynamic inactivation (PDI) has emerged as one promising technology that can alleviate the microbial challenges facing food systems (Cossu et al., 2021; Ghate et al., 2019; Zhu et al., 2021). Although a vast majority of photodynamic studies are in the medical field, application of PDI in food to combat food-related pathogenic and spoilage microorganisms has gained increasing attention from researchers, as indicated by the increasing number of publications in the past 10 years (Fig. S1). A few reviews have summarized the application of PDI to improve the microbiological safety of different food matrixes (Cossu et al., 2021; Ghate et al., 2019; Zhu et al., 2021); however, the impact of PDI on food quality, the commercial niche of this technology, as well as the concerns over the safety of PDI has not been well-addressed. In addition, a comprehensive and in-depth exploration of the antimicrobial mechanisms of PDI in food systems is still missing. To promote and facilitate the future research and application of PDI, the objective of this review is to address this need and provide an up-to-date summary about the recent research progress on the principles, food-related applications, antimicrobial mechanisms, and microbial responses of PDI. To do so, PDI research articles in the areas of food safety and quality control as well as papers studying the PDI antimicrobial mechanisms available in the Web of Science Core Collection published from 2010 to 2020 are reviewed.

## 2. Principles of PDI

In the classic paradigm, PDI comprises three major components: a photosensitizer (PS), light, and molecular oxygen ($^3O_2$) (Fig. 1). PDI occurs when the PS gets excited by the resonant wavelength of light and transits from the ground state ($^0$PS) to a higher energy singlet state ($^1$PS*), which can either return to the ground state and release energy in the form of fluorescence light or undergo an intersystem crossing (ISC) process involving an electronic spin-flip transition to a relatively long-lived excited triplet state ($^3$PS*) (Baptista, Cadet, et al., 2017). $^3$PS* can return to the ground state by releasing the extra energy through phosphorescence or transferring the energy to molecular oxygen ($^3O_2$) through type II reaction to form the excited-state singlet oxygen ($^1O_2$) (Baptista, Cadet, et al., 2017). On the other hand, $^3$PS* can undergo the type I reaction in the presence of an electron donor to form a PS radical anion ($PS^{-}\bullet$), which can react with oxygen to generate superoxide radical anion ($O_2^{-}\bullet$) (Baptista, Cadet, et al., 2017). Both radicals can further react with neighboring molecules to generate hydrogen peroxide ($H_2O_2$) and hydroxyl radical (HO•) (Baptista, Cadet, et al., 2017). $^1O_2$, $O_2^{-}\bullet$, $H_2O_2$, HO• are collectively referred to as reactive oxygen species (ROS). Recently, a potential oxygen-independent type III photochemical pathway was proposed by Hamblin and Abrahamse (2020). The authors identified three examples of oxygen-independent PDI, including the use of psoralens and tetracyclines as PS and the addition of inorganic salts (Hamblin & Abrahamse, 2020).

Two types of PS are involved in PDI, either individually or simultaneously. Many bacteria and fungi species naturally contain endogenous photosensitizers such as porphyrins, flavins, nicotinamide adenine dinucleotide (NADH), and cytochromes (Wang et al., 2021). Of these, porphyrins are the most studied and they have a peak absorption band (the Soret band) at about 400 nm (Ghate et al., 2019). The synthesis of endogenous PS can be effectively increased by adding δ-aminolevulinic acid (ALA), a natural precursor of heme, in growth medium (Ghate et al., 2019).

The addition of exogenous PS can promote the efficiency and application of PDI by shortening the irradiation time or expanding the choices of effective wavelengths. The short half-life of ROS and the fact that it can only exert localized action requires exogenous PS to be in intimate contact with cellular targets (Luksiene, 2021). However, intracellular uptake is not required for PDI; PS remaining outside of the cellular target can still achieve photokilling through the *in situ* generation of ROS (Luksiene, 2021). The main target under this scenario may be restricted to the bacterial and fungal cell wall (Alves et al., 2014; Luksiene, 2021). Once the PS is uptaken by the target cells, PDI could be more effective, as the generated ROS could oxidize critical intracellular components such as the DNA, enzymes, membranes, and lipids, leading to faster and more efficient bacterial and fungal inactivation (Alves et al., 2014; Luksiene, 2021).

The properties of the PS, together with the cell wall structure, determine the uptake process of PS. Cell wall of Gram-positive bacteria consists of a thick but porous layer of peptidoglycan and negatively charged teichoic and lipoteichoic acids (George et al., 2009). Gram-negative bacteria, on the other hand, process an additional well-organized outer membrane rich in negatively charged lipopolysaccharide (LPS) stabilized by cationic ions such as $Mg^{2+}$ or $Ca^{2+}$

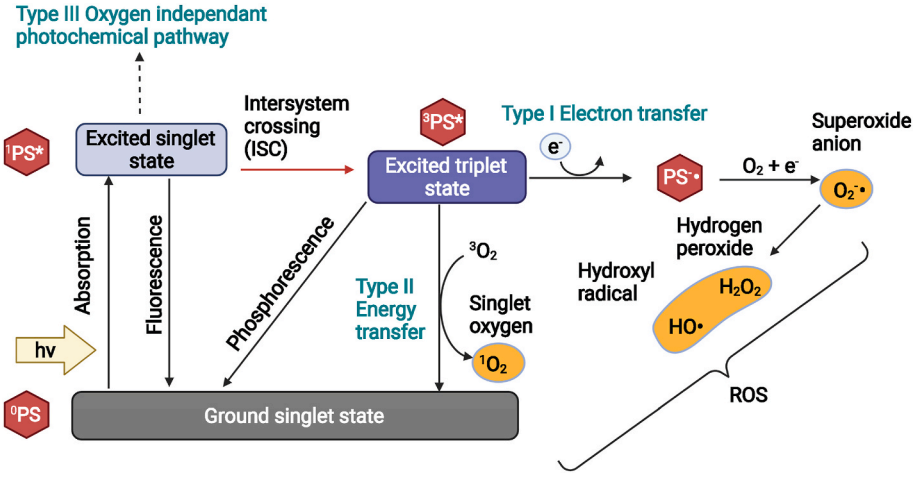


**Fig. 1.** Photosensitization processes in PDI. Ground state photosensitizer ($^0$PS) can be excited by light (hν) at certain wavelength and transit to a higher energy singlet state ($^1$PS*). The short-lived $^1$PS* can either return to the ground state $^0$PS through fluorescence emission or undergo an intersystem crossing (ISC) process to a relatively long-lived excited triplet state ($^3$PS*). $^3$PS* can undergo type II reaction in which it transfers energy to oxygen ($^3O_2$) and produces produce singlet oxygen ($^1O_2$). $^3$PS* can also undergo type I reaction in which it acquires electrons from the surrounding substrates to form free radicals including superoxide radical anion ($O_2^{-}\bullet$), hydrogen peroxide ($H_2O_2$), and hydroxyl radical (HO•). $^1O_2$, $O_2^{-}\bullet$, $H_2O_2$, HO• are collectively referred to as reactive oxygen species (ROS). A potential oxygen-independent type III photochemical pathway was recently proposed. This figure is created with BioRender.com.

(George et al., 2009). Fungal cell wall contains a moderately porous layer of chitin, β-glucan, and mannan, which has an overall negative/neutral charge and an intermediate permeability between Gram-positive and Gram-negative bacteria (Luksiene, 2021). For bacteria, the uptake or binding of neutral and anioinc PS are commonly believed to be inferior to cationic PS, which could be intracellularly accumulated through both electrostatic interactions and self-promoted uptake pathways (George et al., 2009). Similarly, negatively charged fungal cell wall favors the interaction with cationic PS due to electrostatic interactions (Luksiene, 2021).

## 3. Application of PDI in food systems

### 3.1. PDI conditions and antimicrobial efficacy

PDI can effectively control pathogenic and spoilage microorganisms in a variety of food including fresh produce, aquaculture products, and animal products. Although both PDI with and without the use of exogenous PS have been evaluated, most of the studies have focused on the application of exogenous PS (Tables S1 and S2). The most used wavelengths are 405 nm and 395 nm, which are around the wavelength of the maximum absorption (~400 nm) of endogenous PS porphyrins. The most used light source is light-emitting diodes (LEDs), which are semiconductor light devices that emit light with emission wavelengths of narrow bandwidths (D'Souza et al., 2015). The advantages of LED over traditional light sources include no heat generation particularly when exogenous PS are used, the wide range of emission wavelength, compact sizes, high luminous efficacy, and long life expectancy and durability (D'Souza et al., 2015).

Although endogenous PS-mediated PDI can decrease pathogenic and spoilage bacteria and fungi in food, it is worth noting that the exposure duration in most of these studies is hours or even days, particularly in ready-to-eat food (RTE) (Table S1). Such a long exposure time can be problematic if the RTE food products can support the growth of microorganisms. Kim et al. (2017) evaluated the impact of 405-nm LED on the survival of *S.* Enteritidis on the surface of cooked chicken breast at an abuse temperature of 10 °C. After 48 h, even though *S.* Enteritidis populations on illuminated samples were 1–2 log CFU/cm$^2$ lower than those on the control, they were still 1–2 log CFU/cm$^2$ higher than the initial inoculation level. Increasing the treatment temperature to 20 °C further promoted bacterial growth and compromised the antimicrobial efficacy of light (Kim et al., 2017). In addition, for packaged food, prolonged exposure may result in photochemical depletion of oxygen (Ożóg et al., 2019).

To overcome the low inactivation rate of endogenous PS-mediated PDI, PS has been added to food matrixes. Key desirable characteristics of exogenous PS for food applications include the absence of toxic residues to the consumer, minimal impacts on the organoleptic properties of food, and limited costs to produce the molecule. The most-often used exogenous PS is curcumin (Cossu et al., 2021). The same observation is also apparent in Table S2, which shows that 23 (56%) studies applied curcumin as the endogenous PS. It has mostly been dissolved in ethanol and diluted to be applied onto fruits (e.g. apples, cherries, dates, grapes, strawberries, and melon), vegetables (e.g. tomatoes, cucumbers, peppers, spinach, lettuce, maze, seeds, and mung beans), aquaculture products (e.g. oysters, sturgeons, and RTE salted jellyfish), and animal products (e.g. cheese, chicken, beef, pork, and cooked sausage). The second and the third most used are chlorophyllin and hypericin. Vitamins such as riboflavin (VB2) and vitamin K3 are also gaining increasing popularity. The advantages of these natural PS are low toxicity, reduced treatment time, broad-spectrum antimicrobial effect, and prolonged efficacy. The illumination duration in most of the studies reviewed was several minutes to 1 h. For example, Li, et al. (2022) reported that application of 40 mg/ml VK3 water-soluble analogue followed by UV-A or simulated sunlight exposure for 15–30 min reduced the disease incidence of *Penicillium digitatum* inoculated oranges from 100% to 33% and 0%, respectively, after 5 days of incubation at ambient temperature in dark. Kingsley et al. (2018) found that PDI treatment mediated by 0.1% riboflavin and 405-nm LED reduced Tulane virus on blueberries by 0.51 log PFU/ml after 30 min of exposure. Additional discussion about the antimicrobial effect of PDI in different food matrixes can be found in several recent reviews (Cossu et al., 2021; Ghate et al., 2019; Zhu et al., 2021).

### 3.2. Factors impacting PDI efficacy

The efficacy of PDI in food decontamination is determined by various factors, among which food matrix, PS concentration, exposure time, and target microorganisms are the most evaluated. In general, the antimicrobial efficacy of PDI increases with the increase of PS concentration and illumination duration. Delivery methods (e.g., application pattern, incubation time) of exogenous PS can also impact PDI efficacy. Modes of application include immersion, spraying, aerosolization, coating, and packaging. de Oliveira et al. (2018) compared two deposition methods (spraying versus aerosolization) of 10 mg/l acidified curcumin followed by 5 min of UV-A (329–400 nm) exposure of fresh produce. They found that although both methods can reduce *E. coli* O157:H7 inoculated on spinach, lettuce, and tomatoes by ~3 log CFU/cm$^2$, aerosolization resulted in a more uniform deposition of curcumin solution at 1/10 of the volume needed in the spraying method (de Oliveira et al., 2018). Incubation time refers to the treatment time of PS and target microorganisms before light exposure. Buchovec et al. (2016) found that the inactivation of *S.* Typhimurium in saline by using a chlorophyllin-chitosan complex and 405-nm LED increased with the increase of incubation time from 0 to 60 min. Tao et al. (2019), however, found that an incubation time of 10–30 min had no impact on the efficacy of PDI mediated by curcumin and 420-nm LED against generic *E. coli* on fresh-cut apples. Other influencing factors, including the physiochemical properties of PS (e.g., color, solubility, amphipathy, electrical property, reactivity, and stability), characteristics of light (e.g., wavelength, irradiance, and fluence), and properties of the food matrix (e.g., density, turbidity, opacity, organic load, and oxygen concentration) have been discussed by Cossu et al. (2021).

Target microorganisms also play an important role in PDI efficacy, such as fungi versus bacteria, Gram-negative versus Gram-positive bacteria, planktonic cells versus biofilm cells, vegetative cells versus endospores, and enveloped versus non-enveloped viruses. In general, fungi are less susceptible to PDI than bacteria because of the larger size and lower risk of DNA damage in the presence of a nuclear membrane (Luksiene, 2021). It is well-known that Gram-positive bacteria are more sensitive to PDI than Gram-negative bacteria because of differences in cell wall structure, and biofilm cells are more resistant to PDI than planktonic cells because of the protection of extracellular polymeric substances. Luksiene and Paskeviciute (2011) evaluated the antimicrobial efficacy of chlorophyllin-mediated PDI against planktonic cells, biofilms, and endospores of *L. monocytogenes* and *Bacillus cereus* on the surface of the food packaging material polyolefine. They found that 5 min of exposure to 405-nm LED in the presence of 7.5 μM Na-chlorophyllin reduced planktonic cells of *L. monocytogenes* or *B. cereus* by more than 4 log CFU/cm$^2$. Increasing the Na-chlorophyllin concentrations to 75 μM and 150 μM also reduced *B. cereus* spores and *L. monocytogenes* biofilms by more than 4 log CFU/cm$^2$, respectively. In addition, enveloped viruses are more sensitive to PDI than non-enveloped viruses because of their phospholipid and protein coat (Willis et al., 2021).

### 3.3. Impact of PDI treatment on food quality

Most of the food-related studies have reported no negative impact of PDI on food quality (Tables S1 and S2). Shelf-life extension is the most reported positive impact of PDI on food quality. With the use of different exogenous PS, the extension of shelf-life after PDI treatments has been

reported in dates, grapes, strawberries, tomatoes, oysters, sturgeons, and RTE salted jellyfish.

Additional benefits of PDI on food quality include maintenance of quality parameters, preservation of sensory qualities, and reduction of microbial spoilage. For instance, Liu, et al. (2016) found that curcumin-based photosensitization of oysters at 10 μM and 470 nm for 90 s delayed the formation of total volatile basic nitrogen (TVB-N), which is a freshness indicator. The treated oysters also achieved higher sensory scores in odor, color, mucus appearance, texture, pallium gill filaments, and shell muscles after 14 days of storage at 4 °C (Liu et al., 2016). Mukherjee et al. (2020) evaluated visible light irradiation for 2 h a day on *F. oxysporum* artificially inoculated on tomatoes coated with TiO2 nanoparticles co-doped with nitrogen and fluorine. This intermittent PDI completely inhibited the fungal infection on tomatoes compared with control samples (Mukherjee et al., 2020).

However, several studies did observe negative changes in food quality after PDI treatment. The main negative impact of PDI on product quality is temperature increase. In PDI treatments without the use of exogenous PS, temperature increases of food products have been widely reported, and the changes vary greatly depending on the food products, exposure distance, and exposure duration. Increases of 1–4 °C have been reported in fresh-cut pineapple, fresh-cut mango, RTE salmon, and milk (Table S1). However, Subedi, et al. (2020) reported that LED light exposure at 395 nm and 455 nm for 60 min at an exposure distance of 2 cm increased the surface temperature of wheat flour from 25 °C to 86.1 °C and 81 °C, respectively. The temperature increases caused by PDI treatments with the use of exogenous PS were generally more controllable and were typically less than 5 °C (Table S2).

Another main negative impact of PDI treatment on food quality is color change, particularly in PDI without exogenous PS (Table S1). For example, Hyun and Lee (2020) showed that color differences in treated sliced cheeses increased as the illumination time increased. No significant color change was observed from 1 h to seven days when illumination treatment and storage was carried out at 4 °C, while color change values of treated cheese samples increased when the treatments and storage were carried out at 25 °C (Hyun & Lee, 2020).

### 3.4. Commercial importance and potential of PDI

As shown in Tables S1 and S2, majority of the PDI studies have been conducted on fresh fruits and vegetables, indicating one of the niche areas in which the application of PDI can be promising. Over the years, despite the tremendous efforts made to ensure fresh produce safety, they have been repeatedly implicated in various foodborne outbreaks and recalls annually (CDC, 2018). This is mainly because that (1) commercially used short-term chemical decontamination methods (chlorine and peroxyacetic acid) have limited antimicrobial efficacy against foodborne pathogens on fresh produce (Sheng & Zhu, 2021); (2) cross-contamination can happen at various stages before consumption from the equipment, personnel, utensils, and other unhygienic food contact surfaces (Sheng & Zhu, 2021); (3) low levels of foodborne pathogens and spoilage microorganisms can grow to a higher level during post-processing storage particularly at abused temperatures (Kim et al., 2017); (4) no additional decontamination methods can be used by consumers besides washing, which unfortunately is inadequate in the removal of pathogenic or indigenous microorganisms on fresh produce (Bhilwadikar et al., 2019). Therefore, additional interventions are still needed for protecting the safety and quality of fresh produce.

PDI has the potential to fill this niche as fresh produce is continuously or intermittently exposed to light at packing facility, retailer, and consumer levels. In addition, PS can be applied on fresh produce through dipping, spraying, and waxing using the existing processing lines. For other food and food products, PS can also be incorporated into packaging. For example, Chen, et al. (2020) coated polyvinyl acetate and curcumin on the surface of polyvinylidene chloride film. Packaging fresh pork in this film followed by white light exposure for 15 min immediately reduced the total aerobic bacteria counts, maintained the inhibitory effect during subsequent storage at 4 °C for nine days, and improved pork quality by slowing down the production of total volatile basic nitrogen and the increase of pH (Chen et al., 2020).

### 3.5. Safety concerns of PDI and potential solutions

Two main concerns over the safety of PDI include the impact of light exposure on human skin and eyes and the consumption and metabolism of PS in human body. As discussed previously, the most used light source has been blue light (Tables S1 and S2). According to the guidelines by the International Commission on Non-ionizing Radiation Protection (ICNIRP), the limit of exposure to blue light is 100 $J/cm^2 \bullet sr$ for about 167 min per day (ICNIRP, 2014). Overexposure can damage the retina and ocular surface as well as induce skin barrier damage and photoaging (Coats et al., 2021). For the light exposure concern, data in Tables S1 and S2 have shown that most of the treatments particularly with exogenous PS does not need prolonged light exposure. If long-time exposure is needed, enclosing the light devices in a confined environment (a storage room or treatment box) can reduce the likelihood of exposing human skin and eye to light damage significantly. Zhang et al. (2019) found that the photoactivity of Vitamin K1-4, as indicated by the production of hydroxyl radical, remained the same even after four cycles of light exposure. This finding, together with the fact that food is constantly exposed to light, suggests intermittent light exposure as an alternative light delivery method of the continuous light exposure. Furthermore, Sheng, et al. (2020) found continuous die-off of common foodborne pathogens on lemon surfaces during post-PDI cold storage, indicating the potential of coupling short-time PDI and cold chain as a hurdle technology to further improve food safety.

For the concerns over the use of PS, most of the PS tested in food matrixes have been natural PS, with curcumin and chlorophyllin being the top two (Tables S1 and S2). Curcumin has been approved by the US Food and Drug Administration (FDA) as Generally Recognized As Safe (GRAS) and it can be used as an ingredient in food at 0.5–100 mg/100 g (FDA). The joint FAO/WHO Expert Committee on Food Additives (JECFA) specified the Acceptable Daily Intake (ADI) of curcumin is 0–3 mg/kg body weight (JECFA, 2005). Bioavailability of curcumin in human is very low or undetectable due to its poor absorption, rapid metabolism, and systemic elimination; clinical studies have proven the safety of curcumin at as high as 12 g/day over three months (Gupta et al., 2013). Chlorophyllin is a green food colorant and the ADI for copper complexes of chlorophyllin is 0–15 mg/kg by JECFA (JECFA, 1975). Unlike curcumin which has a long established safety record, EFSA Panel on Food Additives and Nutrient Sources Added to Food suggested to withdraw the current ADI of chlorophyllin due to the lack of reliable pharmacokinetics and toxicity data (EFSA, 2015). However, although natural PS-mediated PDI has the advantage of low toxicity and low microbial resistance (which will be discussed later) over traditional preservatives (Zhu et al., 2021), there are still concerns about the consequences of long-term consumption of PDI-treated food. Additional studies on the safety of PS are needed to facilitate its application in food systems.

## 4. Antimicrobial mechanisms of PDI

The key antimicrobial mechanisms of PDI against planktonic cells include the disruption of single cell structure and function, oxidation of macromolecules, inhibition of quorum sensing, and attenuation of virulence factors (Fig. 2). In addition, PDI can damage biofilms by modulation of the expression of genes in the biofilm's bacterial cells, disruption of the biofilm structure, and subsequent reduction of adherent microorganisms. PDI also damages extracellular polymeric substances, including proteins, extracellular DNA (eDNA), and polysaccharides (Fig. 3).

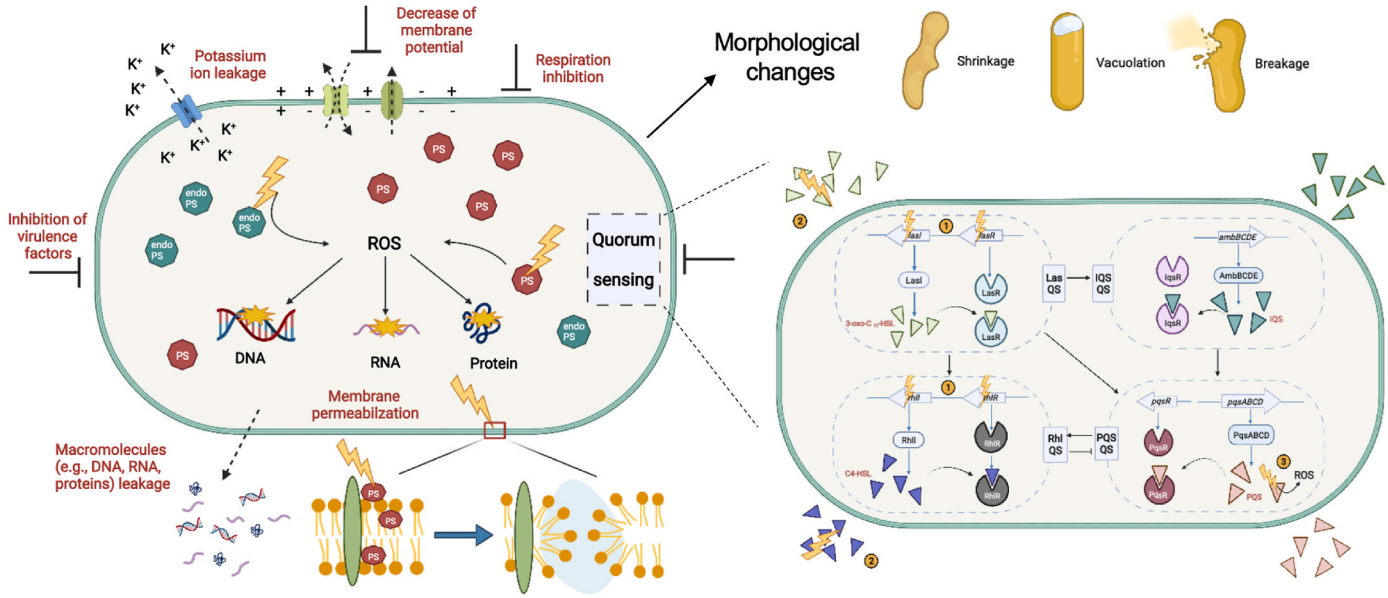


**Fig. 2.** Antimicrobial mechanisms of PDI against planktonic cells using bacteria as a model food-related microorganism. Upon the PDI treatment, direct microscopic observation has shown three major morphologic changes: cell shrinkage, formation of vacuoles, and cell breakage/leakage of intracellular contents. Other structural and functional changes induced by PDI include membrane permeabilization, leakage of macromolecules including proteins and nucleic acids, efflux of potassium ions, reduction of membrane potential, and inhibition of respiration. In addition, PDI can oxidize lipids, proteins, DNA, and RNA through ROS produced by the photosensitization of endogenous and exogeneous PS. Furthermore, PDI inhibits virulence factors through regulating gene expression, reducing their production and activity, and direct inactivation of secreted virulence factors. Lastly, PDI inhibits quorum sensing (QS), one key cell-to-cell communication mechanism for the persistence and survival of microorganisms. Impact of PDI on QS is demonstrated using *Pseudomonas aeruginosa* as an example. *P. aeruginosa* consists at least four interconnected QS systems organized in a multi-layered hierarchy including two AHLs-mediated systems (Las and Rhl systems), *Pseudomonas* quinolone signal (PQS) system, and an integrated QS (IQS) system. PDI can interfere bacterial QS systems through three mechanisms (1) inhibiting the expression of QS-related genes, (2) reducing the secreted QS signaling molecules, and (3) utilizing PQS as an endogenous photosensitizer. This figure is created with BioRender.com.

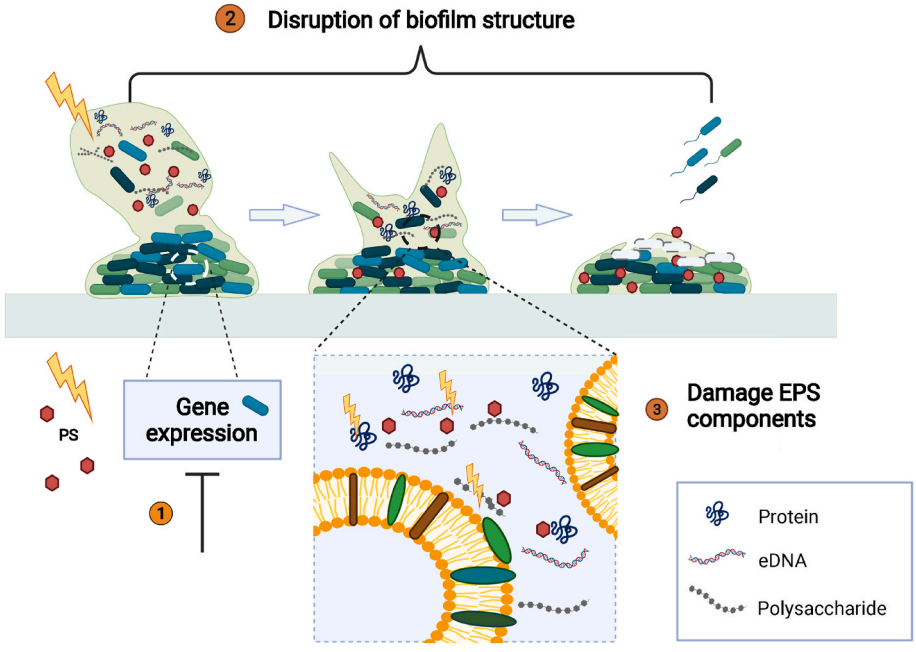


**Fig. 3.** Biofilm disruptive mechanisms of PDI using bacterial biofilm as a model. PDI damages biofilms through (1) modulation of gene expressions of bacterial cells in the biofilm, (2) disruption of biofilm structure and subsequent dispersion/reduction of adherent microorganisms, and (3) damage of extracellular polymeric substance (EPS) components including proteins, extracellular DNA, and polysaccharides. This figure is created with BioRender.com.

### *4.1. Disruption of the structure and functionality of microorganisms*

Many studies report that PDI causes damage to the cellular structure of microorganisms, including morphological changes, membrane permeabilization, leakage of intracellular contents, and disruption of membrane functions (Table 1). The commonly observed morphological changes of single cells include shrinkage or roughening, vacuolation, and cell breakage with or without the release of intracellular components. Microscopic techniques used for the observation of cell morphology include scanning electron microscopy (SEM), transmission

**Table 1**
Impacts of PDI on cell structures and functions of food-related microorganisms.

| Microorganism | Exogenous photosensitizer (PS) | PS treatment system | Light | Observation | Reference |
|---|---|---|---|---|---|
| Disruption of cell structures by microscopic observation | | | | | |
| *Listeria monocytogenes* | NA | NA | LED, 460–470 nm | TEM images showed vacuum formation inside the cells, rough cell wall, blurry cell membrane, disruption of cellular structure, and release of intracellular component. | Hyun and Lee (2020) |
| *Pseudomonas fluorescens* | NA | NA | LED, 460–470 nm | TEM images showed shrunken cell membrane and the release of intracellular components | Hyun and Lee (2020) |
| *Saccharomyces cerevisiae* | NA | NA | Coherent Chameleon Vision II mode-locked femtosecond Ti:sapphire laser, 830 nm (two-photon excitation) | Confocal images showed expulsion of the cellular content | Grangeteau et al. (2018) |
| *Escherichia coli* O157:H7 | Vitamin K3 | Tryptic soy broth | UV-A at 320–400 nm or simulated sunlight at 300–400 nm | SEM images showed the formation of filamentous cells and the reduction of extracellular flagella/fimbriae | Sheng et al. (2020) |
| *Escherichia coli* (generic) | Tetrakis(N-ethylpyridinium-4-yl)porphyrin tetratosylate | Phosphate buffered saline | LED, blue, 400–415 nm | TEM images showed the formation of vacuoles, and leakage of intracellular contents | Pudziuvyte et al. (2011) |
| *Listeria monocytogenes* | Vitamin K3 | Tryptic soy broth | UV-A at 320–400 nm or simulated sunlight at 300–400 nm | SEM images showed cell breakage | Sheng et al. (2020) |
| | Titanium dioxide | Quartz tube | UVB, 306 nm | SEM images showed cell breakage | Kim et al. (2013) |
| | Methylene blue | Phosphate buffered saline | Tungsten halogen LHT75, visible light | AFM images showed coarse cell membrane and shrunken cell surfaces | Lin et al. (2012) |
| *Salmonella* Enteritidis PT30 | Vitamin K3 | Tryptic soy broth | UV-A at 320–400 nm or simulated sunlight at 300–400 nm | SEM results showed cell breakage and the reduction of extracellular flagella/fimbriae | Sheng et al. (2020) |
| *Salmonella* Typhimurium | Titanium dioxide | Quartz tube | UVB, 306 nm | SEM images showed cell breakage | Kim et al. (2013) |
| *Staphylococcus aureus* | Curcumin | Luria-Bertani (LB) broth with dimethyl sulfoxide | LED, blue, 470 nm | TEM images showed vacuolation inside the cells | Jiang et al. (2014) |
| *Vibrio parahaemolyticus* | Methylene blue | Phosphate buffered saline | Photocatalysis-xenon lamp | TEM images showed the release of intracellular contents | Deng et al. (2016) |
| *Penicillium expansum* | Curcumin | Sterile water | LED, 420 nm | SEM and TEM images showed shrunken and broken cell wall, vacuolation, cytoplasmic efflux, and obscure organelles and nuclear envelope | Song et al. (2020) |
| **Increased cell wall/membrane permeability** | | | | | |
| *Escherichia coli* (generic) *Staphylococcus aureus* | NA | NA | LED, 405 nm | Epifluorescence microscopic images showed increased numbers of cells stained with SYTOX, a nucleic acid stain that only penetrates cells with compromised membranes | McKenzie et al. (2016) |
| *Escherichia coli* O157:H7 *Salmonella* Typhimurium *Shigella sonnei* | NA | NA | LED, 405 nm | Epifluorescence microscopic images showed increased numbers of cells stained with propidium iodide (PI), a nucleic acid stain that penetrates cells with compromised membranes | Kim et al. (2016) |
| *Listeria monocytogenes* *Pseudomonas fluorescens* | NA | NA | LED, 460–470 nm | PDI treatment induced PI uptake through the measurement of fluorescence | Hyun and Lee (2020) |
| *Saccharomyces cerevisiae* | NA | NA | Coherent Chameleon Vision II mode-locked femtosecond Ti:sapphire laser, 830 nm (two-photon excitation) | Confocal microscopic images showed that PDI treatment induced the efflux of singlet oxygen sensor green, a fluorescence probe that can't penetrate intact membrane | Grangeteau et al. (2018) |
| *Escherichia coli* (generic) | Polyacrylamide-polydopamine/Ag@AgCl | Hydrogel | Xenon lamp | PDI treated bacteria showed higher absorbance at 420 nm after incubation with o-nitrophenyl-β-galactoside, which is a chromogenic substrate for detection of β-galactosidase activity | Mao et al. (2019) |
| | Tetrakis(N-ethylpyridinium-4-yl)porphyrin tetratosylate | Phosphate buffered saline | LED, blue, 400–415 nm | Enzymatic assays showed that PDI reduced the activities of periplasmic alkaline phosphatase and cytoplasmic β-galactosidase in bacterial cells, indicating the reduction of outer and inner membrane permeability, respectively | Pudziuvyte et al. (2011) |
| *Fusarium* spp. | | | LED, red, 635 nm | Flow cytometry results showed that PDI induced PI uptake | |

(*continued on next page*)

**Table 1** (*continued*)

| Microorganism | Exogenous photosensitizer (PS) | PS treatment system | Light | Observation | Reference |
|---|---|---|---|---|---|
| | Methylene blue, toluidine blue O, and new methylene blue N | Phosphate buffered saline | | | de Menezes et al. (2016) |
| *Candida albicans* | New methylene blue N or pentacyclic compound S137 | Water | LED, red, 631 nm | Confocal fluorescence microscopy images showed that PDI induced PI uptake | Rodrigues et al. (2020) |
| **Leakage of cellular contents** | | | | | |
| *Escherichia coli* (generic)<br>*Staphylococcus aureus* | NA | NA | LED, 405 nm | Absorbance of bacteria supernatants at 260 nm following light exposure increased with the increase of light dose, indicating that PDI induced the leakage of nucleic acids | McKenzie et al. (2016) |
| *Enterococcus hirae* | Rose Bengal or erythrosine | Phosphate buffered saline | LED, green, 530 nm | Flame emission and atomic absorption spectroscopy analysis of cell-free supernatant showed that PDI treatment resulted in leakage of potassium (K+) | Silva et al. (2018) |
| *Escherichia coli* (generic) | Rose Bengal or erythrosine | Phosphate buffered saline | LED, green, 530 nm | PDI caused leakage of K+ through analysis of bacterial supernatant by flame emission and atomic absorption spectroscopy | Silva et al. (2018) |
| | Polyacrylamide-polydopamine/Ag@AgCl | Hydrogel | Xenon lamp | The Bicinchoninic Acid Protein (BCA) assay showed increased leakage of protein from bacteria after PDI | Mao et al. (2019) |
| | Tetrakis(N-ethylpyridinium-4-yl)porphyrin tetratosylate | Phosphate buffered saline | LED, blue, 400–415 nm | PDI induced the leakage of nucleic acids and total protein as increased amount of protein (BCA assay) and 260-nm absorbing compounds were observed in the supernatant; Measurement of tetraphenylphosphonium ion (TPP+) concentration in the bacterial suspension by a TPP + electrode indicated that PDI reduced bacterial membrane potential | Pudziuvyte et al. (2011) |
| *Staphylococcus aureus* | Polyacrylamide-polydopamine/Ag@AgCl | Hydrogel | Xenon lamp | BCA assay showed increased leakage of protein from bacteria after PDI | Mao et al. (2019) |
| | Rose Bengal or erythrosine | Phosphate buffered saline | LED, green, 530 nm | PDI caused leakage of K+ through analysis of bacterial supernatant by flame emission and atomic absorption spectroscopy | Silva et al. (2018) |
| | Rose Bengal, phloxine B, erythrosine B, porphyrin | Phosphate buffered saline | Halogen lamp | Analysis of bacterial suspension using K+ and TPP + electrodes showed that PDI induced the leakage of K+ and reduced membrane potential, respectively | Kato et al. (2018) |
| *Listeria innocua* | Rose Bengal or erythrosine | Phosphate buffered saline | LED, green, 530 nm | PDI caused leakage of K+ through analysis of bacterial supernatant by flame emission and atomic absorption spectroscopy | Silva et al. (2018) |
| *Listeria monocytogenes* | Methylene blue | Phosphate buffered saline | Tungsten-halogen LHT75 | Spectrophotometric analysis showed that PDI induced the leakage of 260 nm and 270 nm absorbing materials | Lin et al. (2012) |
| **Inhibition of respiration** | | | | | |
| *Escherichia coli* (generic) | Tetrakis(N-ethylpyridinium-4-yl)porphyrin tetratosylate | Phosphate buffered saline | LED, blue, 400–415 nm | Measurement with a high resolution respirometry oxygraph showed that PDI inhibited bacterial oxygen consumption | Pudziuvyte et al. (2011) |
| *Staphylococcus aureus* | Rose Bengal, phloxine B, erythrosine B, porphyrin | Phosphate buffered saline | Halogen lamp | PDI reduced oxygen consumption of bacteria as measured by oxygen electrode | Kato et al. (2018) |

NA: not available; LED: light-emitting diode; AFM: atomic force microscopy; SEM: scanning electron microscopy; TEM: transmission electron microscopy.

electron microscopy (TEM), and atomic force microscopy (AFM). Among them, SEM and TEM are the most used techniques.

To confirm the microscopic observations, measurements of membrane permeability were conducted to evaluate membrane integrity by monitoring the influx of membrane-impermeable chemicals (e.g., propidium iodide, SYTOX green) and efflux of intracellular contents (e.g., potassium ion, proteins, nucleic acids). For example, exposure to the red LED light at 635 nm in the presence of methylene blue, toluidine blue O, new methylene blue N, and phenothiazinium derivative S137 significantly increased the uptake of propidium iodide in the microconidia of *F. oxysporum, F. moniliforme,* and *F. solani* (de Menezes et al., 2016). Co-incubation of *E. coli* and *S. aureus* with polyacrylamide-polydopamine/Ag@AgCl hydrogels followed by illumination under a xenon lamp resulted in significantly increased release of total protein and cytoplasmic enzyme β-galactosidase to supernatant (Mao et al., 2019). Besides the disruption of cellular structures, PDI also effectively damage the structure of acellular entities, namely viruses. Porphyrin-mediated PDI has been shown to target viral envelopes resulting in irregular structures (Neris et al., 2018). Although not common, Majiya, Adeyemi, Herod, et al. (2018) found that porphyrin-mediated PDI damaged capsid integrity of type 1 murine norovirus.

In addition to cell structure and integrity, PDI also damages cell functionality. For instance, illumination of *S. aureus* under halogen lamp in the presence of porphyrin, rose Bengal, phloxine B, and erythrosine B significantly reduced bacterial membrane potential (Kato et al., 2018), which is crucial for various bacterial functions. Pudziuvyte et al. (2011) found that blue light irritation of generic *E. coli* in the presence of porphyrin derivative inhibited bacterial respiration by reducing oxygen consumption.

The ability of PDI to disrupt cell integrity and functionality is affected by several factors, including light dose, PS concentration and physiochemical properties, structure of the cell wall, as well as treatment temperatures. For example, in the presence of 0.5 μg/ml methylene blue, the leakage of protein and nucleic acids of *L. monocytogenes* increased in proportion to the irradiation time (Lin et al., 2012). Upon blue LED exposure with porphyrin-based PS, the respiration efficacy of *E. coli* decreased rapidly with increasing concentrations of porphyrin (Pudziuvyte et al., 2011). Kato et al. (2018) evaluated the impact of structure on porphyrin-induced damage in *S. aureus* under a halogen lamp. The dysfunction of bacterial membrane was observed in the order of protoporphyrin ~ mesoporphyrin > deuteroporphyrin > hematoporphyrin derivative » hematoporphyrin > photofrin > coprocorphyrin ~ uroporphyrin. In general, Gram-negative bacteria are more resistant to photodynamic damage to cell structure than Gram-positive bacteria (Luksiene, 2021). Conflicting results have been reported about the influence of treatment temperature. Mao et al. (2019) observed more severe damage to morphology, membrane permeability, and protein leakage in both *E. coli* and *S. aureus* when the photodynamic treatment temperature was increased to 52.1 °C, while more severe morphological damage and increased membrane permeability were observed at 4 °C than 25 °C in both *L. monocytogenes* and *P. fluorescens* (Hyun & Lee, 2020).

### 4.2. Damage of macromolecules

Damage caused by PDI on the macromolecules, including protein, lipids, and nucleic acid, of food-related microorganisms is summarized in Table 2. Proteins are believed to be the major targets of PDI-induced oxidation because of their abundance (e.g. 50–55% of the dry weight of *E. coli* and 35–60% of the dry weight of *S. cerevisiae*) and vital functions (Alves et al., 2014).

#### 4.2.1. Proteins

PDI-induced protein oxidation has been reported in a wide range of microorganisms (bacteria, yeasts, molds, and viruses) using different quantification methods, such as sodium dodecyl sulfate (SDS)-polyacrylamide gel electrophoresis (PAGE) analysis, immunoblotting, protein carbonyl assay, infrared spectroscopy, and proteomics. SDS-PAGE is the most used method to analyze the changes of protein profile. Besides the overall damage, PDI also induces functional damages to proteins. Baptista, Sabino, et al. (2017) utilized Fourier transform infrared spectroscopy (FT-IR) and found that PDI mediated by 50 μM methylene blue and red LED at 662 nm downgraded C═C, C═N, C═O, and N═N of proteins and amides in yeast *Candida albicans* (Baptista, Sabino, et al., 2017). However, these damages were mainly observed in lag-phase cells; more pronounced degradation of polysaccharides and lipids was observed in stationary-phase cells (Baptista, Sabino, et al., 2017). Majiya, Adeyemi, Stonehouse, and Millner (2018) assessed the impact of PDI mediated by porphyrin derivative 5,10,15,20-tetrakis(1-methyl-4--pyridinio) porphyrin tetra *p*-toluenesulfonate (TMPyP) and cool white light on the host recognition and attachment protein (A-protein) of bacteriophage MS2, a commonly used surrogate for human norovirus. The authors first illuminated MS2 for 1–60 min with 1 μM TMPyP and then conducted western blot with sequence-specific antibodies targeting four selected antigenic regions of the A-protein. Two antibodies failed to detect A-protein after 1 min of PDI and the other two after 10 min, indicating the potential role of PDI in the loss of virus antigenicity.

A more comprehensive analysis of PDI-induced changes in microbial protein profile can be achieved through proteomic approach. Dosselli et al. (2012) applied a classic proteomic assay, including two-dimensional gel electrophoresis and mass spectrometry analysis, to identify the specific membrane proteins of *S. aureus* that were damaged in sub-lethal PDI mediated by *meso*-tetra (4-N-methyl-pyridyl) porphine and light exposure at 390–460 nm. They found that PDI markedly affected proteins involved in energy metabolism, oxidative stress response, cell division, and sugar uptake. For example, KatA, a catalase involved in detoxification, was induced by up to 7.87-fold; expression of chaperone protein DnaK, which is involved in protein synthesis, was reduced to one fifth of that in the control (Dosselli et al., 2012). A recent study by Chang et al. (2020) applied liquid chromatography(LC)/mass spectrometry (MS)/MS-based shotgun proteomic approach to explore modified proteins in the PDI treatment of *Acinetobacter baumannii* mediated by curcumin and blue light. Analysis of proteins specifically carbonylated under PDI showed the top two categories were membrane proteins and translation-involving proteins (Chang et al., 2020).

The exact photo-induced damage to proteins occurs through multiple pathways. Firstly, a small number of amino acid residues, particularly tryptophan, tyrosine, histidine, and disulfide residues, can directly absorb incident radiation, resulting in the formation of free radicals (Pattison et al., 2012). Secondly, the free radicals formed in the type I PDI react with proteins to form side-chain radicals and backbone radicals, which induce several propagation reactions and result in the formation of various products, such as α-carbon hydroperoxide, side-chain hydroperoxide, side-chain hydroxides/alcohols, and carbonyl compounds (Pattison et al., 2012). Finally, singlet oxygen formed in the type II PDI can cause oxidative damages to cysteine, methionine, histidine, tyrosine, tryptophan, and cystine (Pattison et al., 2012). The consequences of these processes include formation of protein peroxide, side-chain products, cross-links, and aggregates, protein unfolding, backbone fragmentation, and enzyme inactivation (Pattison et al., 2012).

#### 4.2.2. Lipids

Unsaturated lipids in cell membranes are well-known targets of photosensitized oxidation. In type I PDI, free radicals react with unsaturated lipids and trigger a chain peroxidation cascade involving various products; photo-peroxidation induced by type II PDI is less complex, and $^1O_2$ reacts with the proximal lipids to form lipid hydroperoxide (Di Mascio et al., 2019). PDI has been reported to oxidize membrane phospholipids in both bacteria and fungi, including generic *E. coli*, *Enterococcus faecium*, *Pseudomonas aeruginosa*, *S. aureus* and *P. expansum,*

**Table 2**
Impacts of PDI on macromolecules of food-related microorganisms.

| Microorganism | Exogenous photosensitizer (PS) | PS treatment system | Light | Observation | Reference |
|---|---|---|---|---|---|
| Proteins | | | | | |
| *Acinetobacter baumannii* | Curcumin | Luria-Bertani broth with dimethyl sulfoxide | LED, blue | Proteomic analysis showed that PDI caused carbonylation of proteins related to the membrane structure, translation, and responses to oxidative stress | Chang et al. (2020) |
| *Escherichia coli* (generic) | 5,10,15,20-tetrakis(1-methylpyridinium-4-yl)porphyrin tetra-iodide | Phosphate buffered saline with dimethyl sulfoxide | OSRAM lamp, white light, 380–700 nm | Sodium dodecyl sulfate (SDS)-polyacrylamide gel electrophoresis (PAGE) showed that PDI induced large scale protein degradation | Alves et al. (2015) |
| *Listeria monocytogenes* | Methylene blue | Phosphate buffered saline | Tungsten halogen LHT75, visible light | SDS-PAGE analysis showed that PDI induced large scale degradation of proteins | Lin et al. (2012) |
| *Pseudomonas aeruginosa* | Methylene blue | Phosphate buffered saline | PDT-1200 lamp, 560–780 nm | SDS-PAGE showed no significant change in outer membrane profile; 2-D electrophoresis showed a change in the expression of outer membrane protein following PDI | Shih and Huang (2013) |
| *Staphylococcus aureus* | *meso*-tetra (4-N-methyl-pyridyl) porphine | Phosphate buffered saline | UV 236 lamp, 390–460 nm | Proteomic analysis showed that PDI impacted the expression of several functional classes of proteins, most of which were involved in metabolic activities, oxidative stress responses, cell division, and the uptake of sugar | Dosselli et al. (2012) |
| *Staphylococcus warneri* | 5,10,15,20-tetrakis(1-methylpyridinium-4-yl)porphyrin tetra-iodide | Phosphate buffered saline with dimethyl sulfoxide | OSRAM lamp, white light, 380–700 nm | SDS-PAGE analysis showed that PDI induced large scale degradation of proteins | Alves et al. (2015) |
| *Vibrio parahaemolyticus* | Curcumin | Phosphate buffered saline with ethanol | LED, 470 nm | SDS-PAGE analysis showed that PDI reduced protein bands extracted from the bacterial outer membrane | Wu et al. (2016) |
| *Penicillium expansum* (spores) | Curcumin | Water | LED, 420 nm | Measurement of protein carbonyl showed that PDI induced protein oxidation in spores | Song et al. (2020) |
| *Candida albicans* | Methylene blue | Phosphate buffered saline | LED, 662 nm | Fourier transform infrared (FTIR) spectroscopy analysis showed that PDI degraded C═C, C═N, C═O, and N═N of proteins and amides | Baptista, Sabino, et al. (2017) |
| Herpes simplex virus | Orthoquin | Dulbecco's modified Eagle's medium with dimethyl sulfoxide | LED, visible light | Immunoblotting results showed that PDI physically disrupted virus structural proteins | Monjo et al. (2018) |
| Bacteriophage MS2 | 5,10,15,20-tetrakis(1-methyl-4-pyridinio) porphyrin tetra *p*-toluenesulfonate | Phosphate buffered saline | Schott KL 2500 LCD, cool white light | Western blot and native agarose gel electrophoresis results showed that PDI induced crosslinking of virus coat proteins and the loss of antigenicity of A-protein, the host recognition and the attachment protein within the virus capsid | Majiya, Adeyemi, Stonehouse, and Millner (2018) |
| | Carbon dots with 2,2'-(ethylenedioxy) bis(ethylamine) | Tryptic soy broth | Visible light | SDS-PAGE showed that PDI had no impact on the total amount of viral coat proteins; protein carbonyl assay showed that PDI induced protein oxidation | Dong, Edmondson, et al. (2020) |
| **Lipids** | | | | | |
| *Escherichia coli* (generic) | Tricationic porphyrin | Phosphate buffered saline with dimethyl sulfoxide | Artificial white light, 380–700 nm | Lipidomic analysis showed that PDI significantly increased the concentration of lipid hydroperoxides, decreased the unsaturated C16:1 and C18:1 fatty acids, induced the oxidation of phosphatidylethanolamines with C16:1, C18:1, and C18:2 fatty acyl chains, and the formation of hydroxy and hydroperoxyl derivatives | Alves, Santos, et al. (2013) |
| | Porphyrin derivatives | Phosphate buffered saline with dimethyl sulfoxide | Artificial white light, 380–700 nm | Lipidomic analysis showed that PDI induced lipid peroxidation, increased the proportion of saturated C16:0 fatty acid and decreased monounsaturated fatty acid C18:1N9, and decreased the overall relative concentration of unsaturated fatty acids | Lopes et al. (2014) |
| *Enterococcus faecium* | Oligomeric polyethylenimine-carbon dots | Phosphate buffered saline | LED, visible light | PDI induced lipid peroxidation by quantifying malondialdehyde (MDA) with the thiobarbituric acid reactive substances assay (TBARS) | Dong, Ge, et al. (2020) |
| *Pseudomonas aeruginosa Staphylococcus aureus* | Toluidine blue-carbon nanotube conjugate | Luria-Bertani broth | Diode laser, red, 670 nm | TBARS results showed that PDI induced lipid peroxidation | Anju et al. (2019) |
| *Staphylococcus warneri* | Tricationic porphyrin | Phosphate buffered saline | Artificial white light, 380–700 nm | Lipidomic analysis showed that PDI induced the modification of membrane phospholipids (increased phosphatidylglycerols and decreased | Alves, Melo, et al. (2013) |

(*continued on next page*)

**Table 2** (*continued*)

| Microorganism | Exogenous photosensitizer (PS) | PS treatment system | Light | Observation | Reference |
|---|---|---|---|---|---|
| | | with dimethyl sulfoxide | | cardiolipins) and the formation of lipid hydroperoxides and hydroxides | |
| *Penicillium expansum* | Curcumin | Water | LED, 420 nm | Measurement of MDA by Microscale Malondialdehyde assay kit showed that PDI induced the lipid peroxidation of spores | Song et al. (2020) |
| **Nucleic acids** | | | | | |
| *Staphylococcus aureus* | NA | Tryptic soy broth | LED, blue, 470 nm | Fourier transform infrared (FTIR) spectroscopy results indicated that PDI induced changes in DNA conformation | Bumah et al. (2017) |
| | New methylene blue, Toluidine blue O, 5,10,15,20-tetrakis(1-methyl-4-pyridinio) porphyrin tetra (*p*-toluenesulfonate), zinc phthalocyanine, Rose Bengal, or no exogenous PS | | LED at 627 nm or 405 nm, Light® PDT lamp at 620–780 nm or 385–480 nm | Agarose gel electrophoresis results showed that PDI with and without exogenous PS degraded DNA | Grinholc et al. (2015) |
| *Vibrio parahaemolyticus* | Curcumin | Phosphate buffered saline with ethanol | LED, 470 nm | Agarose gel electrophoresis showed that PDI degraded DNA and RNA | Wu et al. (2016) |
| *Candida albicans* | Methylene blue | Phosphate buffered saline | LED, 662 nm | FTIR spectroscopy results showed that PDI caused degradation of functional groups related to C–O of deoxyribose, C–C of DNA; C–O stretching vibration of C–OH group of ribose-RNA; P–O stretching modes originated from phosphodiester groups of nucleic acids | Baptista, Sabino, et al. (2017) |
| Bacteriophage MS2 | Carbon dots with 2,2'-(ethylenedioxy) bis(ethylamine) | Tryptic soy broth | Visible light | Agarose gel electrophoresis results showed that PDI degraded genomic RNA | Dong, Edmondson, et al. (2020) |
| Type 1 murine norovirus | 5, 10, 15, 20-tetrakis (1-methyl-4-pyridinio) porphyrin- tetra- p-toluene sulfonate | Phosphate buffered saline | Cool white light, 400–786 nm | RNA transfection demonstrated that PDI reduced the infectivity of genome of RNA virus | Majiya, Adeyemi, Herod, et al. (2018) |

NA: not available; LED: light-emitting diode.

through the quantification of malondialdehyde generated from lipid peroxidation (Anju et al., 2019; Dong, Ge, et al., 2020; Lopes et al., 2014; Song et al., 2020).

A few studies systematically evaluated photodynamic oxidation of bacterial membranes using lipidomics. For example, Alves, Melo, et al. (2013) assessed the impact of PDI using a tricationic porphyrin and artificial white light at 380–700 nm on the lipid profile of *Staphylococcus warneri*. They found that the major phospholipids in *S. warneri* were phosphatidylglycerols (PGs, ~50%) and cardiolipins (CLs, ~20%). After PDI treatment, large amounts of hydroperoxides were formed. Further analysis proved that the oxidative products mainly came from CLs, which contain unsaturated fatty acyl chains, while fatty acid composition of PGs are mostly saturated acyl chains (Alves, Melo, et al., 2013). Unlike Gram-positive bacteria such as *S. warneri*, the major phospholipid classes in Gram-negative *E. coli* are phosphatidylethanolamines (PEs, 53%), followed by 40% PGs and 7% CLs (Alves, Santos, et al., 2013). Tricationic porphyrin-mediated PDI under white light induced the oxidation of PEs with C16:1, C18:1, and C18:2 fatty acyl chains and resulted in the formation of hydroxy and hydroperoxyl derivatives (Alves, Santos, et al., 2013). In addition, the degree of lipid oxidation is dependent on the number and position of positive charges on porphyrin derivatives, with two to four positive charges more effective in oxidizing unsaturated fatty acids in *E. coli* than one positive charge (Lopes et al., 2014). Interestingly, although large amounts of lipid hydroperoxides are formed during photosensitization, PDI-induced membrane permeabilization is likely due to a very low percentage of lipid aldehydes formed by the interaction of phospholipids with free radicals (Bacellar et al., 2018).

#### 4.2.3. Nucleic acids

These oxidative damages of both isolated and cellular DNA are measured by immunoassays, enzymatic assays, gas chromatography-mass spectrometry (GC-MS), high performance liquid chromatography-electrochemical detection (HPLC-ECD), HPLC-MS, and HPLC-MS/MS (Cadet et al., 2017). Among all pyrimidine and purine DNA bases, guanine is the preferable target of $^1O_2$ (Di Mascio et al., 2019). In food-related microorganisms, Grinholc, et al. (2015) observed DNA smears on agarose gel in *S. aureus* treated with 405 nm light alone, 627-nm LED with 50 μM new methylene blue, 100 μM toluidine blue O, or 100 μM TMPyP, 620–780 nm red light with 5 μM zinc phthalocyanine, or 385–480 nm blue light with 5 μM rose Bengal. FT-IR spectroscopy results showed that blue light irradiation at 470 nm induced C–C stretching of the DNA backbone and base-pairing vibration of DNA in *S. aureus* (Bumah et al., 2017).

Although limited, studies have also demonstrated the PDI-induced damages on the abundance, conformation, and functionality of RNA in food-related microorganisms. Wu et al. (2016) found that light exposure at 470 nm for 1 min in the presence of 10 μM curcumin abolished the RNA bands of *Vibrio parahaemolyticus*. However, this cannot be solely explained by PDI damages, as bacterial populations after the aforementioned treatment were reduced by more than 6 log CFU/ml. Baptista, Sabino, et al. (2017) reported that PDI mediated by 662-nm LED and 50 μM methylene blue degraded functional groups related to C–O stretching vibration of the C–OH group of ribose-RNA in the pathogenic yeast *C. albicans*. Majiya, Adeyemi, Herod, et al. (2018) evaluated the impact of TMPyP and cool white light (400–786 nm) on the genome of type 1 murine norovirus, a non-enveloped RNA virus. Since the genome of RNA viruses alone is infectious if introduced to susceptible cells, the authors first treated the virus with PDI, and then extracted and purified the RNA, which was then transfected into BHK-21 cells. The combination of 5 μM TMPyP and 10 min of exposure markedly reduced the RNA infectivity, indicating the damage caused by PDI on the viral genome (Majiya, Adeyemi, Herod, et al., 2018).

### 4.3. Inhibition of quorum sensing (QS)

QS is a cell-to-cell communication mechanism by which microorganisms produce, detect, and respond to extracellular signaling molecules (Barriuso et al., 2018). QS has been reported in bacteria, viruses, fungi, and parasites, among which bacterial QS is the most widely

studied (Barriuso et al., 2018; Bassler & Losick, 2006). A wide range of signaling molecules is involved in bacterial QS, such as N-acyl homoserine lactones (AHLs) produced by Gram-negative bacteria, oligopeptides produced by Gram-positive bacteria, and autoinducer-2 (AI-2) produced by both Gram-negative and Gram-positive bacteria (Bassler & Losick, 2006).

In general, PDI can interfere with bacterial QS systems through three mechanisms: (1) inhibiting the expression of QS-related genes, (2) reducing the secreted QS signaling molecules, and (3) utilizing QS signaling molecules as photosensitizers (Table 3). The signaling network in *P. aeruginosa* is one of the best studied and most complex known QS systems. *P. aeruginosa* consists of at least four interconnected QS systems organized in a multi-layered hierarchy, including two AHLs-mediated systems (Las and Rhl systems), a *Pseudomonas* quinolone signal (PQS) system, and an integrated QS signal (IQS) system (Lee & Zhang, 2015). The signaling molecules are *N*-3-oxo-dodecanoyl homoserine lactone (3-oxo-$C_{12}$-HSL), *N*-butanoyl homoserine lactone ($C_4$-HSL), PQS, and IQS, which are produced by LasI, RhlI, PqsABCD, and AmbBCDE and recognized by LasR, RhlR, PqsR, and IqsR, respectively (Lee & Zhang, 2015). The Las system, which is at the top of the hierarchy, activates three other QS systems as well as the corresponding virulence genes (Lee & Zhang, 2015).

PDI has been repeatedly reported to suppress the expression of genes involved in the Las and Rhl systems of *P. aeruginosa*. For example, a recent study found that blue light (405 nm) irradiation at 10 J/cm$^2$ in the presence of 6.75 mM curcumin markedly suppressed the expression of *lasI, lasR, rhlI,* and *rhlR* (Abdulrahman et al., 2020). In addition, Fila et al. (2018) found that blue light treatment at 411 nm and 150 J/cm$^2$ significantly decreased the activity of 3-oxo-$C_{12}$-HSL and $C_4$-HSL while having no impact on PQS activity. The 3-oxo-$C_{12}$-HSL of the Las system and the $C_4$-HSL of the Rhl system are AHL-based signaling molecules that are typically composed of an invariant homoserine lactone ring acylated at the amino nitrogen by a fatty acid chain of 4–18 carbons (Lee & Zhang, 2015). PQS is chemically different from the AHLs and is identified as 2-heptyl-3-hydroxy-4-quinolone; quinolone is one of the typical photosensitizers (Lee & Zhang, 2015). In fact, UV-A (365 nm) exposure of PQS extracted from *P. aeruginosa* induced the production of singlet oxygen and superoxide anion (Pezzoni et al., 2015).

The impacts of PDI on QS are influenced by many factors, including bacterial strain, light dose, and PS concentration. For example, among 12 *P. aeruginosa* strains, UV-A treatment at 365 nm and 150 J/cm$^2$ significantly reduced the production of 3-oxo-$C_{12}$-HSL and $C_4$-HSL in five and seven strains, respectively (Pezzoni et al., 2015). The combination of 6.75 mM curcumin and 405-nm blue light irradiation at 5 and 10 J/cm$^2$ reduced *lasI* expression in *P. aeruginosa* by ~10% and 60%, respectively (Abdulrahman et al., 2020). When *P. aeruginosa* was exposed to 108 J/cm$^2$ red light at 630 nm, 5-aminolevulinic acid at 20 mM caused significantly more reductions in the expression of the *lasI*, *lasR*, *rhlI*, and *rhlR* genes compared with the reductions at 10 mM (Tan et al., 2018).

### 4.4. Disruption of biofilm

Biofilm is defined as an aggregate of microorganisms embedded in a matrix of self-produced extracellular polymeric substance (EPS) adhere to a surface or to each other (de Melo et al., 2013). Bacteria, yeasts, and filamentous fungi can form biofilms (de Melo et al., 2013). A recent review by Wang et al. (2021) summarized the antibiofilm mechanisms of PDI, which include the modulation of gene expression in the microorganisms in the biofilm, dispersion/reduction of adherent microorganisms, and reduction of EPS components including polysaccharides, proteins, and eDNA. The antibiofilm efficacy of PDI is influenced by light engineering variables, structure and concentration of PS, biofilm characteristics (e.g., age, thickness, structure, single-/mixed-species), contact surface (e.g., texture, hydrophobicity, charge), and food environment (Wang et al., 2021).

Although most studies are on single-species biofilms, mixed-species biofilms are the most common form in nature (de Melo et al., 2013). Conflicting results have been reported about the sensitivity of single- and mixed-species biofilms to PDI (Wang et al., 2021). The formation of cross-kingdom biofilms further complicates the situation due to the intricate interactions (synergistic or antagonistic) between bacteria and yeast (*Candida*) (Pereira et al., 2011). Cross-kingdom biofilms are generally more resistant to PDI than single-species bacterial or fungal biofilms (Pereira et al., 2011). It's worth noting that lethal PDI occurred mainly in the upper layer of biofilms and microorganisms in the lower layer could remain alive (Zhang et al., 2017). Therefore, additional disruptive strategies are needed to better remove the biofilms. Potential hurdle strategies such as organic acids, enzymes, EDTA, biosurfactant, nanobubble and nanocarriers can facilitate the disruption of biofilm structure and penetration of PS and oxygen (Wang et al., 2021).

**Table 3**
Impacts of PDI on quorum sensing (QS) of food-related microorganisms.

| Microorganism | Exogenous photosensitizer (PS) | PS treatment system | Light | Main finding | Reference |
|---|---|---|---|---|---|
| *Pseudomonas aeruginosa* | Curcumin | Distilled water with dimethyl sulfoxide | 405 nm, blue | PDI reduced the expression of *lasI, lasR, rhlI,* and *rhlR*, which encode LasI synthase, transcriptional regulator LasR, RhlI synthase, and transcriptional regulator RhlR, respectively | Abdulrahman et al. (2020) |
| | Indocyanine green | Distilled water | Diode laser, 810 nm | PDI reduced *lasI* expression | Pourhajibagher et al. (2020) |
| | 5-Aminolevulinic acid | Phosphate buffered saline | LED, 630 nm | PDI reduced the expression of *lasI, lasR, rhlI,* and *rhlR* | Tan et al. (2018) |
| | NA | NA | Single-emitter diode lamp, blue, 411 nm | PDI reduced the AHLs-based QS molecules while had no impact on *Pseudomonas* quinolone signal | Fila et al. (2018) |
| | NA | NA | Ultraviolet A, 365 nm | *Pseudomonas* quinolone signal acted as an endogenous PS | Pezzoni et al. (2015) |
| *Staphylococcus aureus* | Indocyanine green | Distilled water | Diode laser, 810 nm | PDI reduced the expression of *agr*, which encodes the QS accessory gene regulator (Agr) system | Pourhajibagher et al. (2020) |
| *Acinetobacter baumannii* | Indocyanine green | Distilled water | Diode laser, 810 nm | PDI reduced the expression of *abaI,* which involves in the production of AHLs and biofilm formation | Pourhajibagher et al. (2020) |
| *Enterococcus faecalis* | C-Phycocyanin | Brain heart infusion broth | Diode laser, 635 nm | PDI down-regulated QS gene *fsrB* | Pourhajibagher et al. (2020) |
| *Serratia marcescens* | Methylene blue | Phosphate buffered saline | LED, 660 nm | PDI down-regulated *swrR,* which encodes AHLs-dependent regulator | Fekrirad et al. (2019) |

NA: not available; LED: light-emitting diode; AHLs: acyl-homoserine lactones.
[1]Ampicillin was incorporated into the hollow carbon nitride sphere as an additional hurdle.

### 4.5. Virulence factors

PDI inhibits virulence factors through regulating gene expression, reducing the production and activity of virulence factors, or direct inactivation of secreted virulence factors (Table 4). For example, Ogonowska and Nakonieczna (2020) found that a 10-min treatment with 0.25 μM rose Bengal followed by green light exposure at 515 nm for 40 min reduced the expression of *seb* encoding the Staphylococcal enterotoxin B by 2.8 $\log_2$ fold. Fekrirad et al. (2019) found that the hemolysin production of *S. marcescens* strains that survived the PDI treatment of 50 μM methylene blue in combined with 660-nm LED light exposure was reduced by up to 57.6%. Illumination under white light at 380–700 nm in the presence of 5 μM porphyrin derivative completely inactivated Staphylococcal isolated enterotoxins A and C (Bartolomeu et al., 2016). Reduced potency of secreted virulence factors of *P. aeruginosa* post-PDI treatment has also been confirmed with a human keratinocyte cell line (Fila et al., 2017).

The anti-virulence properties of PDI are influenced by the PS concentration and light dose. For instance, red light illumination at 632 nm in the presence of 5 μM new methylene blue decreased the *seb* expression in *S. aureus* by ~1.2 and 1.9 $\log_2$ unit after 20 and 40 min, respectively (Ogonowska & Nakonieczna, 2020). At a fixed light dose of 108 J/cm$^2$ using 630-nm red LED, treatment with 10 and 20 nM 5-aminolevulinic acid reduced the pyocyanin production of *P. aeruginosa* by 13.3% and 49.4%, respectively (Tan et al., 2018).

## 5. Potential development of tolerance, persistence, or resistance to PDI

Like other antimicrobial strategies currently used by the food industry, PDI in most cases cannot fully eliminate pathogenic or spoilage microorganisms in food (Tables S1 and S2). In this case, the survivors, which have been exposed to oxidative stress, elicit a variety of adaptive responses that can potentially impact their innate antimicrobial susceptibility (Alves et al., 2014). The oxidative stress responses in bacteria have been extensively reviewed and mainly include production of protective pigments, activation of efflux pumps that can pump out PS, activation of redox-sensitive transcriptional regulators (e.g., OxyR, SoxRS, PerR), increased production of antioxidant enzymes (e.g., superoxide dismutases, catalases, and peroxidases), activation of $\sigma^E$ (RpoE) that modulates the expression of heat shock σ-factors and subsequent production of heat shock protein (e.g., GroESL, DnaK), initiation of DNA repair (e.g., SOS response, excision repair), and entry into a viable but nonculturable (VBNC) state (Alves et al., 2014).

There are different types of antimicrobial susceptibility, including tolerance, persistence, and resistance. According to Brauner et al. (2016), "resistance" describes the inherited ability of microorganisms to grow at high concentrations of antimicrobials (e.g., antibiotics). "Tolerance" describes the ability of microorganisms (inherited or not) to survive a temporary exposure to high concentrations of antimicrobials (Brauner et al., 2016). Unlike tolerance and resistance, which describe the whole populations, "persistence" describes the ability of a subpopulation of a clonal population to survive high concentrations of antimicrobials (Brauner et al., 2016). Possible persistence in pathogenic bacteria after PDI treatment has been reported. Forte Giacobone et al. (2016) evaluated the survival of *P. aeruginosa* irradiated with red LED at ~630 nm for 0–240 min in the presence of methylene blue (MB). When the concentration of MB was at 6 μM, a decrease in the slope of the survival curve was observed. Further increasing the initial MB concentrations to 30 μM or addition of 15 μM MB after 150 min of exposure failed to improve the lethal effect of PDI. These findings ruled out the influence of MB photodecomposition on tailing of the survival curve, indicating the presence of a small subpopulation with increased tolerance to MB-mediated PDI (Forte Giacobone et al., 2016).

To answer the question of whether food-related microorganisms can develop tolerance or resistance to PDI, numerous studies have been conducted. Target microorganisms have been treated by PDI, survivors have been regrown, and the same PDI treatment has been repeated for several cycles. Overall, PDI treatment at lethal (>3 log reductions) or sublethal (1–2 log reductions) conditions with and without exogenous PS did not induce resistance in bacteria (generic *E. coli*, *S. aureus*, *A. baumannii*, *P. aeruginosa*, and *E. faecalis*), yeast (*C. albicans*), or virus (T3-like phage) after 4–25 cycles of treatment because of its ROS-driven and multi-targeted mode of action (Rapacka-Zdończyk et al., 2021). A few studies, however, did report increased tolerance after consecutive cycles of PDI exposure. For example, Rapacka-Zdończyk et al. (2021) found that *S. aureus* developed tolerance to sublethal PDI consisting of 0.1 μM rose Bengal and illumination with 515-nm LED at 10 J/cm$^2$ (RB-PDI) and blue light alone at 411 nm (BL) after five cycles of photo-treatments. The developed tolerance was specific to each treatment; in other words, RB-PDI (BL) tolerance was induced only with the sublethal RB-PDI (BL) treatment. The tolerance was stable, as the susceptibility of *S. aureus* originated from the 10th consecutive cycle was not different than that of *S. aureus* from the 10th cycle followed by five cycles of subculturing without selection pressure (sublethal RB-PDI or BL treatment) (Rapacka-Zdończyk et al., 2021).

**Table 4**
Impacts of PDI on virulence factors of food-related microorganisms.

| Microorganism | Exogenous photosensitizer (PS) | PS treatment system | Light | Main finding | Reference |
|---|---|---|---|---|---|
| *Pseudomonas aeruginosa* | 5-Aminolevulinic acid | Phosphate buffered saline | LED, red, 630 nm | PDI inhibited the expression of *rhlA* (involved in the synthesis of virulence factor rhamnolipid) and *lasB* (encoding the virulence factor LasB elastase) and the secretion of pyocyanin and elastase | Tan et al. (2018) |
| | NA | NA | Single-emitter diode lamp, blue, 405 nm | PDI inhibited the secretion of pyocyanin, elastase A (staphylolysin), elastase B (pseudolysin), and other proteases | Fila et al. (2017) |
| *Staphylococcus aureus* | New methylene blue | Milli-Q water | LED, red, 632 nm | PDI reduced the expression of *seb* encoding Staphylococcal enterotoxin B, one of the toxins involved in staphylococcal food poisoning | Ogonowska and Nakonieczna (2020) |
| | Rose Bengal | Milli-Q water | LED, green, 515 nm | PDI reduced *seb* expression | Ogonowska and Nakonieczna (2020) |
| | 5,10,15,20-tetrakis(1-methylpyridinium-4-yl) porphyrin tetra-iodide | Phosphate buffered saline with dimethyl sulfoxide | White light, 380–700 nm | PDI inactivated secreted enterotoxins A and C, which are the staphylococcal food poisoning causative agents | Bartolomeu et al. (2016) |
| *Serratia marcescens* | Methylene blue | Phosphate buffered saline | LED, 660 nm | PDI reduced prodigiosin production, hemolysin activity, swimming and swarming motility, and the expression of the flagellar gene *flhD* | Fekrirad et al. (2019) |

NA: not available; LED: light-emitting diode.

## 6. Conclusion and perspectives

As presented in this review, PDI with exogenous PS can effectively control pathogenic and spoilage bacteria, fungi, spores, and viruses in a variety of foods, including fruits, vegetables, aquaculture products, and animal products, as well as on food contact surfaces. The efficacy of PDI is influenced by multiple factors, including the physiochemical properties of PS, characteristics of the light, the food matrix, and the target microorganisms. The antimicrobial mode of action of PDI is multi-targeted, including the disruption of cell wall structures and functions, oxidation of macromolecules (e.g., proteins, lipids, and nucleic acids), inhibition of quorum sensing, disruption of biofilm, and damage of virulence factors. Therefore, microorganisms are unlikely to develop resistance to PDI.

To facilitate the deployment of PDI in the food industry, additional efforts are still needed in following aspects, including exploring novel PS with desirable properties (e.g. low toxicity, high efficacy, renewability, low cost, and water solubility), evaluation of the impact of PS on human health, optimization of PDI systems (e.g. novel PS delivery methods, cost-effective light sources/devices, and solar energy), and challenge studies at pilot or commercial scale. Besides the optimization in PDI parameters, in-depth understanding of the antimicrobial mechanisms of PDI can further support its application. Studies toward the specificity of its mode of action and the mechanisms for the potential development of tolerance or resistance are still needed.

## Funding information

Authors thank the funding support received from the National Institute of Food and Agriculture, United States Department of Agriculture (Grant # 2019-06980).

## Appendix A. Supplementary data

Supplementary data to this article can be found online at https://doi.org/10.1016/j.tifs.2022.04.001.

## References

Abdulrahman, H., Misba, L., Ahmad, S., & Khan, A. U. (2020). Curcumin induced photodynamic therapy mediated suppression of quorum sensing pathway of *Pseudomonas aeruginosa*: An approach to inhibit biofilm *in vitro*. *Photodiagnosis and Photodynamic Therapy, 30*, Article 101645.

Alves, E., Esteves, A. C., Correia, A., Cunha, Â., Faustino, M. A., Neves, M. G., & Almeida, A. (2015). Protein profiles of *Escherichia coli* and *Staphylococcus warneri* are altered by photosensitization with cationic porphyrins. *Photochemical and Photobiological Sciences, 14*, 1169–1178.

Alves, E., Faustino, M. A., Neves, M. G., Cunha, A., Tome, J., & Almeida, A. (2014). An insight on bacterial cellular targets of photodynamic inactivation. *Future Medicinal Chemistry, 6*, 141–164.

Alves, E., Melo, T., Simões, C., Faustino, M. A. F., Tomé, J. P. C., Neves, M. G. P. M. S., Cavaleiro, J. A. S., Cunha, Â., Gomes, N. C. M., Domingues, P., Domingues, M. R. M., & Almeida, A. (2013). Photodynamic oxidation of *Staphylococcus warneri* membrane phospholipids: New insights based on lipidomics. *Rapid Communications in Mass Spectrometry, 27*, 1607–1618.

Alves, E., Santos, N., Melo, T., Maciel, E., Dória, M. L., Faustino, M. A., Tomé, J. P., Neves, M. G., Cavaleiro, J. A., Cunha, Â., Helguero, L. A., Domingues, P., Almeida, A., & Domingues, M. R. (2013). Photodynamic oxidation of *Escherichia coli* membrane phospholipids: New insights based on lipidomics. *Rapid Communications in Mass Spectrometry, 27*, 2717–2728.

Anju, V. T., Paramanantham, P., B, S., L, S., Sharan, A., Syed, A., Bahkali, N. A., Alsaedi, M. H., Kaviyarasu, K., & Busi, S. (2019). Antimicrobial photodynamic activity of toluidine blue-carbon nanotube conjugate against *Pseudomonas aeruginosa* and *Staphylococcus aureus* - understanding the mechanism of action. *Photodiagnosis and Photodynamic Therapy, 27*, 305–316.

Bacellar, I. O. L., Oliveira, M. C., Dantas, L. S., Costa, E. B., Junqueira, H. C., Martins, W. K., Durantini, A. M., Cosa, G., Di Mascio, P., Wainwright, M., Miotto, R., Cordeiro, R. M., Miyamoto, S., & Baptista, M. S. (2018). Photosensitized membrane permeabilization requires contact-dependent reactions between photosensitizer and lipids. *Journal of the American Chemical Society, 140*, 9606–9615.

Baptista, M. S., Cadet, J., Di Mascio, P., Ghogare, A. A., Greer, A., Hamblin, M. R., Lorente, C., Nunez, S. C., Ribeiro, M. S., Thomas, A. H., Vignoni, M., & Yoshimura, T. M. (2017). Type I and Type II photosensitized oxidation reactions: Guidelines and mechanistic pathways. *Photochemistry and Photobiology, 93*, 912–919.

Baptista, A., Sabino, C. P., Núñez, S. C., Miyakawa, W., Martin, A. A., & Ribeiro, M. S. (2017). Photodynamic damage predominates on different targets depending on cell growth phase of *Candida albicans*. *Journal of Photochemistry and Photobiology B: Biology, 177*, 76–84.

Barriuso, J., Hogan, D. A., Keshavarz, T., & Martínez, M. J. (2018). Role of quorum sensing and chemical communication in fungal biotechnology and pathogenesis. *FEMS Microbiology Reviews, 42*, 627–638.

Bartolomeu, M., Rocha, S., Cunha, Â., Neves, M. G., Faustino, M. A., & Almeida, A. (2016). Effect of photodynamic therapy on the vrulence factors of *Staphylococcus aureus*. *Frontiers in Microbiology, 7*, 267.

Bassler, B. L., & Losick, R. (2006). Bacterially speaking. *Cell, 125*, 237–246.

Bhilwadikar, T., Pounraj, S., Manivannan, S., Rastogi, N. K., & Negi, P. S. (2019). Decontamination of microorganisms and pesticides from fresh fruits and vegetables: A comprehensive review from common household processes to modern techniques. *Comprehensive Reviews in Food Science and Food Safety, 18*, 1003–1038.

Brauner, A., Fridman, O., Gefen, O., & Balaban, N. Q. (2016). Distinguishing between resistance, tolerance and persistence to antibiotic treatment. *Nature Reviews Microbiology, 14*, 320–330.

Buchovec, I., Lukseviciute, V., Marsalka, A., Reklaitis, I., & Luksiene, Z. (2016). Effective photosensitization-based inactivation of Gram (−) food pathogens and molds using the chlorophyllin–chitosan complex: Towards photoactive edible coatings to preserve strawberries. *Photochemical and Photobiological Sciences, 15*, 506–516.

Bumah, V. V., Aboualizadeh, E., Masson-Meyers, D. S., Eells, J. T., Enwemeka, C. S., & Hirschmugl, C. J. (2017). Spectrally resolved infrared microscopy and chemometric tools to reveal the interaction between blue light (470nm) and methicillin-resistant *Staphylococcus aureus*. *Journal of Photochemistry and Photobiology B: Biology, 167*, 150–157.

Cadet, J., Davies, K. J. A., Medeiros, M. H. G., Di Mascio, P., & Wagner, J. R. (2017). Formation and repair of oxidatively generated damage in cellular DNA. *Free Radical Biology and Medicine, 107*, 13–34.

CDC. (2018). National outbreak reporting system (NORS). https://wwwn.cdc.gov/norsdashboard/. (Accessed 30 April 2020).

Chang, K.-C., Cheng, Y.-Y., Lai, M.-J., & Hu, A. (2020). Identification of carbonylated proteins in a bactericidal process induced by curcumin with blue light irradiation on imipenem-resistant *Acinetobacter baumannii*. *Rapid Communications in Mass Spectrometry, 34*, Article e8548.

Chen, L., Song, Z., Zhi, X., & Du, B. (2020). Photoinduced antimicrobial activity of curcumin-containing coatings: Molecular interaction, stability and potential application in food decontamination. *ACS Omega, 5*, 31044–31054.

Coats, J. G., Maktabi, B., Abou-Dahech, M. S., & Baki, G. (2021). Blue light protection, Part I—effects of blue light on the skin. *Journal of Cosmetic Dermatology, 20*, 714–717.

Cossu, M., Ledda, L., & Cossu, A. (2021). Emerging trends in the photodynamic inactivation (PDI) applied to the food decontamination. *Food Research International, 144*, Article 110358.

D'Souza, C., Yuk, H.-G., Khoo, G. H., & Zhou, W. (2015). Application of light-emitting diodes in food production, postharvest preservation, and microbiological food safety. *Comprehensive Reviews in Food Science and Food Safety, 14*, 719–740.

Deng, X., Tang, S., Wu, Q., Tian, J., Riley, W. W., & Chen, Z. (2016). Inactivation of *Vibrio parahaemolyticus* by antimicrobial photodynamic technology using methylene blue. *Journal of the Science of Food and Agriculture, 96*, 1601–1608.

Dewey-Mattia, D., Manikonda, K., Hall, A. J., Wise, M. E., & Crowe, S. J. (2018). Surveillance for foodborne disease outbreaks - United States, 2009-2015. *MMWR Surveillance Summaries, 67*, 1–11.

Di Mascio, P., Martinez, G. R., Miyamoto, S., Ronsein, G. E., Medeiros, M. H. G., & Cadet, J. (2019). Singlet molecular oxygen reactions with nucleic acids, lipids, and proteins. *Chemical Reviews, 119*, 2043–2086.

Dong, X., Edmondson, R., Yang, F., Tang, Y., Wang, P., Sun, Y.-P., & Yang, L. (2020a). Carbon dots for effective photodynamic inactivation of virus. *RSC Advances, 10*, 33944–33954.

Dong, X., Ge, L., Abu Rabe, D. I., Mohammed, O. O., Wang, P., Tang, Y., Kathariou, S., Yang, L., & Sun, Y.-P. (2020). Photoexcited state properties and antibacterial activities of carbon dots relevant to mechanistic features and implications. *Carbon, 170*, 137–145.

Dosselli, R., Millioni, R., Puricelli, L., Tessari, P., Arrigoni, G., Franchin, C., Segalla, A., Teardo, E., & Reddi, E. (2012). Molecular targets of antimicrobial photodynamic therapy identified by a proteomic approach. *Journal of Proteomics, 77*, 329–343.

Doyle, M. P., & Buchanan, R. L. (2013). *Food microbiology: Fundamentals and frontiers* (4th ed.). Washington, DC: ASM Press.

EFSA. (2015). Scientific opinion on re-evaluation of copper complexes of chlorophylls (E 141(i)) and chlorophyllins (E 141(ii)) as food additives. *EFSA Journal, 13*, 4151.

FAO. (2018a). Sustainable food systems, concept and frame work. http://www.fao.org/3/ca2079en/CA2079EN.pdf. (Accessed 7 September 2021).

FAO. (2019a). *The State of Food and Agriculture 2019. Moving forward on food loss and waste reduction*. Rome: Licence: CC BY-NC-SA 3.0 IGO.

FDA. (2018b). Hazard analysis critical control point (HACCP). https://www.fda.gov/food/guidance-regulation-food-and-dietary-supplements/hazard-analysis-critical-control-point-haccp. (Accessed 7 February 2022).

FDA. (2019b). GRAS notices GRN No.822. https://www.cfsanappsexternal.fda.gov/scripts/fdcc/?set=GRASNotices&sort=GRN_No&order=DESC&startrow=1&type=basic&search=curcumin. (Accessed 9 February 2022).

Fekrirad, Z., Kashef, N., & Arefian, E. (2019). Photodynamic inactivation diminishes quorum sensing-mediated virulence factor production and biofilm formation of *Serratia marcescens*. *World Journal of Microbiology and Biotechnology, 35*, 191.

Fila, G., Kawiak, A., & Grinholc, M. S. (2017). Blue light treatment of *Pseudomonas aeruginosa*: Strong bactericidal activity, synergism with antibiotics and inactivation of virulence factors. *Virulence, 8*, 938–958.

Fila, G., Krychowiak, M., Rychlowski, M., Bielawski, K. P., & Grinholc, M. (2018). Antimicrobial blue light photoinactivation of *Pseudomonas aeruginosa*: Quorum sensing signaling molecules, biofilm formation and pathogenicity. *Journal of Biophotonics, 11*, Article e201800079.

Forte Giacobone, A. F., Ruiz Gale, M. F., Hogert, E. N., & Oppezzo, O. J. (2016). A possible phenomenon of persistence in *Pseudomonas aeruginosa* treated with methylene blue and red light. *Photochemistry and Photobiology, 92*, 702–707.

George, S., Hamblin, M. R., & Kishen, A. (2009). Uptake pathways of anionic and cationic photosensitizers into bacteria. *Photochemical and Photobiological Sciences, 8*, 788–795.

Ghate, V. S., Zhou, W., & Yuk, H.-G. (2019). Perspectives and trends in the application of photodynamic inactivation for microbiological food safety. *Comprehensive Reviews in Food Science and Food Safety, 18*, 402–424.

Grangeteau, C., Lepinois, F., Winckler, P., Perrier-Cornet, J.-M., Dupont, S., & Beney, L. (2018). Cell death mechanisms induced by photo-oxidation studied at the cell scale in the yeast *Saccharomyces cerevisiae*. *Frontiers in Microbiology, 9*.

Grinholc, M., Rodziewicz, A., Forys, K., Rapacka-Zdonczyk, A., Kawiak, A., Domachowska, A., Golunski, G., Wolz, C., Mesak, L., Becker, K., & Bielawski, K. P. (2015). Fine-tuning *recA* expression in *Staphylococcus aureus* for antimicrobial photoinactivation: Importance of photo-induced DNA damage in the photoinactivation mechanism. *Applied Microbiology and Biotechnology, 99*, 9161–9176.

Gupta, S. C., Patchva, S., & Aggarwal, B. B. (2013). Therapeutic roles of curcumin: Lessons learned from clinical trials. *The AAPS Journal, 15*, 195–218.

Hamblin, M. R., & Abrahamse, H. (2020). Oxygen-independent antimicrobial photoinactivation: Type III photochemical mechanism? *Antibiotics, 9*, 53.

Hyun, J.-E., & Lee, S.-Y. (2020). Antibacterial effect and mechanisms of action of 460–470 nm light-emitting diode against *Listeria monocytogenes* and *Pseudomonas fluorescens* on the surface of packaged sliced cheese. *Food Microbiology, 86*, Article 103314.

ICNIRP. (2014). ICNIRP guidelines on limits of exposure to incoherent visible and infrared radiation: Errata. *Health Physics, 106*, 530–531.

JECFA. (1975). *Toxicological evaluation of some food colors, enzymes, flavor enhancers, thickening agents, and certain food additives.* https://inchem.org/documents/jecfa/jecmono/v06je17.htm. (Accessed 9 February 2022).

JECFA. (2005). Curcumin. https://inchem.org/documents/jecfa/jeceval/jec_460.htm. (Accessed 9 February 2022).

Jiang, Y., Leung, A. W., Hua, H., Rao, X., & Xu, C. (2014). Photodynamic action of LED-activated curcumin against *Staphylococcus aureus* involving intracellular ROS increase and membrane damage, 2014 *International Journal of Photoenergy*, Article 637601.

Kato, H., Komagoe, K., Inoue, T., Masuda, K., & Katsu, T. (2018). Structure-activity relationship of porphyrin-induced photoinactivation with membrane function in bacteria and erythrocytes. *Photochemical and Photobiological Sciences, 17*, 954–963.

Kim, M.-J., Adeline Ng, B. X., Zwe, Y. H., & Yuk, H.-G. (2017). Photodynamic inactivation of *Salmonella enterica* Enteritidis by 405 ± 5-nm light-emitting diode and its application to control salmonellosis on cooked chicken. *Food Control, 82*, 305–315.

Kim, S., Ghafoor, K., Lee, J., Feng, M., Hong, J., Lee, D.-U., & Park, J. (2013). Bacterial inactivation in water, DNA strand breaking, and membrane damage induced by ultraviolet-assisted titanium dioxide photocatalysis. *Water Research, 47*, 4403–4411.

Kim, M.-J., Mikš-Krajnik, M., Kumar, A., & Yuk, H.-G. (2016). Inactivation by 405 ± 5 nm light emitting diode on *Escherichia coli* O157:H7, *Salmonella* Typhimurium, and *Shigella sonnei* under refrigerated condition might be due to the loss of membrane integrity. *Food Control, 59*, 99–107.

Kingsley, D. H., Perez-Perez, R. E., Boyd, G., Sites, J., & Niemira, B. A. (2018). Evaluation of 405-nm monochromatic light for inactivation of Tulane virus on blueberry surfaces. *Journal of Applied Microbiology, 124*, 1017–1022.

Lee, J., & Zhang, L. H. (2015). The hierarchy quorum sensing network in *Pseudomonas aeruginosa*. *Protein & Cell, 6*, 26–41.

Lin, S.-l., Hu, J.-m., Tang, S.-s., Wu, X.-y., Chen, Z.-q., & Tang, S.-z. (2012). Photodynamic inactivation of methylene blue and tungsten-halogen lamp light against food pathogen *Listeria monocytogenes*. *Photochemistry and Photobiology, 88*, 985–991.

Li, X., Sheng, L., Sbodio, A. O., Zhang, Z., Sun, G., Blanco-Ulate, B., & Wang, L. (2022). Photodynamic control of fungicide-resistant *Penicillium digitatum* by vitamin K3 water-soluble analogue. *Food Control, 135*, Article 108807.

Liu, F., Li, Z., Cao, B., Wu, J., Wang, Y., Xue, Y., Xu, J., Xue, C., & Tang, Q. J. (2016). The effect of a novel photodynamic activation method mediated by curcumin on oyster shelf life and quality. *Food Research International, 87*, 204–210.

Lopes, D., Melo, T., Santos, N., Rosa, L., Alves, E., Clara Gomes, M., Cunha, Â., Neves, M. G. P. M. S., Faustino, M. A. F., Domingues, M. R. M., & Almeida, A. (2014). Evaluation of the interplay among the charge of porphyrinic photosensitizers, lipid oxidation and photoinactivation efficiency in *Escherichia coli*. *Journal of Photochemistry and Photobiology B: Biology, 141*, 145–153.

Luksiene, Z. (2021). Photosensitization: Principles and applications in food processing. In K. Knoerzer, & K. Muthukumarappan (Eds.), *Innovative food processing technologies* (pp. 368–384). Oxford: Elsevier.

Luksiene, Z., & Paskeviciute, E. (2011). Microbial control of food-related surfaces: Na-Chlorophyllin-based photosensitization. *Journal of Photochemistry and Photobiology B: Biology, 105*, 69–74.

Majiya, H., Adeyemi, O. O., Herod, M., Stonehouse, N. J., & Millner, P. (2018). Photodynamic inactivation of non-enveloped RNA viruses. *Journal of Photochemistry and Photobiology B: Biology, 189*, 87–94.

Majiya, H., Adeyemi, O. O., Stonehouse, N. J., & Millner, P. (2018b). Photodynamic inactivation of bacteriophage MS2: The A-protein is the target of virus inactivation. *Journal of Photochemistry and Photobiology B: Biology, 178*, 404–411.

Mao, C., Xiang, Y., Liu, X., Zheng, Y., Yeung, K. W. K., Cui, Z., Yang, X., Li, Z., Liang, Y., Zhu, S., & Wu, S. (2019). Local photothermal/photodynamic synergistic therapy by disrupting bacterial membrane to accelerate reactive oxygen species permeation and protein leakage. *ACS Applied Materials & Interfaces, 11*, 17902–17914.

McKenzie, K., Maclean, M., Grant, M. H., Ramakrishnan, P., MacGregor, S. J., & Anderson, J. G. (2016). The effects of 405 nm light on bacterial membrane integrity determined by salt and bile tolerance assays, leakage of UV-absorbing material and SYTOX green labelling. *Microbiology, 162*, 1680–1688.

de Melo, W. C. M. A., Avci, P., de Oliveira, M. N., Gupta, A., Vecchio, D., Sadasivam, M., Chandran, R., Huang, Y. Y., Yin, R., Perussi, L. R., Tegos, G. P., Perussi, J. R., Dai, T. H., & Hamblin, M. R. (2013). Photodynamic inactivation of biofilm: Taking a lightly colored approach to stubborn infection. *Expert Review of Anti-infective Therapy, 11*, 669–693.

de Menezes, H. D., Tonani, L., Bachmann, L., Wainwright, M., Braga, G.Ú. L., & von Zeska Kress, M. R. (2016). Photodynamic treatment with phenothiazinium photosensitizers kills both ungerminated and germinated microconidia of the pathogenic fungi *Fusarium oxysporum, Fusarium moniliforme* and *Fusarium solani*. *Journal of Photochemistry and Photobiology B: Biology, 164*, 1–12.

Monjo, A. L. A., Pringle, E. S., Thornbury, M., Duguay, B. A., Monro, S. M. A., Hetu, M., Knight, D., Cameron, C. G., McFarland, S. A., & McCormick, C. (2018). Photodynamic inactivation of Herpes simplex viruses. *Viruses, 10*, 532.

Mukherjee, K., Acharya, K., Biswas, A., & Jana, N. R. (2020). TiO2 nanoparticles co-doped with nitrogen and fluorine as visible-light-activated antifungal agents. *ACS Applied Nano Materials, 3*, 2016–2025.

Neris, R. L. S., Figueiredo, C. M., Higa, L. M., Araujo, D. F., Carvalho, C. A. M., Verçoza, B. R. F., Silva, M. O. L., Carneiro, F. A., Tanuri, A., Gomes, A. M. O., Bozza, M. T., Da Poian, A. T., Cruz-Oliveira, C., & Assunção-Miranda, I. (2018). Co-protoporphyrin IX and Sn-protoporphyrin IX inactivate Zika, Chikungunya and other arboviruses by targeting the viral envelope. *Scientific Reports, 8*, 9805.

Ogonowska, P., & Nakonieczna, J. (2020). Validation of stable reference genes in *Staphylococcus aureus* to study gene expression under photodynamic treatment: A case study of SEB virulence factor analysis. *Scientific Reports, 10*, Article 16354.

de Oliveira, E. F., Tikekar, R., & Nitin, N. (2018). Combination of aerosolized curcumin and UV-A light for the inactivation of bacteria on fresh produce surfaces. *Food Research International, 114*, 133–139.

Ożóg, Ł., Domka, W., Truszkiewicz, A., Tarbarkiewicz, J., & Aebisher, D. (2019). Monitoring photodynamic oxygen consumption by endogenous oxygen contrast MRI. *Photodiagnosis and Photodynamic Therapy, 25*, 492–498.

Pattison, D. I., Rahmanto, A. S., & Davies, M. J. (2012). Photo-oxidation of proteins. *Photochemical and Photobiological Sciences, 11*, 38–53.

Pereira, C. A., Romeiro, R. L., Costa, A. C. B. P., Machado, A. K. S., Junqueira, J. C., & Jorge, A. O. C. (2011). Susceptibility of *Candida albicans, Staphylococcus aureus*, and *Streptococcus mutans* biofilms to photodynamic inactivation: An in vitro study. *Lasers in Medical Science, 26*, 341–348.

Pezzoni, M., Meichtry, M., Pizarro, R. A., & Costa, C. S. (2015). Role of the *Pseudomonas* quinolone signal (PQS) in sensitising *Pseudomonas aeruginosa* to UVA radiation. *Journal of Photochemistry and Photobiology B: Biology, 142*, 129–140.

Pourhajibagher, M., Mahmoudi, H., Rezaei-soufi, L., Alikhani, M. Y., & Bahador, A. (2020). Potentiation effects of antimicrobial photodynamic therapy on quorum sensing genes expression: A promising treatment for multi-species bacterial biofilms in burn wound infections. *Photodiagnosis and Photodynamic Therapy, 30*, Article 101717.

Pudziuvyte, B., Bakiene, E., Bonnett, R., Shatunov, P. A., Magaraggia, M., & Jori, G. (2011). Alterations of *Escherichia coli* envelope as a consequence of photosensitization with tetrakis(N-ethylpyridinium-4-yl)porphyrin tetratosylate. *Photochemical and Photobiological Sciences, 10*, 1046–1055.

Rapacka-Zdończyk, A., Woźniak, A., Nakonieczna, J., & Grinholc, M. (2021). Development of antimicrobial phototreatment tolerance: Why the methodology matters. *International Journal of Molecular Sciences, 22*, 2224.

Rodrigues, G. B., Brancini, G. T. P., Uyemura, S. A., Bachmann, L., Wainwright, M., & Braga, G. U. L. (2020). Chemical features of the photosensitizers new methylene blue N and S137 influence their subcellular localization and photoinactivation efficiency in *Candida albicans*. *Journal of Photochemistry and Photobiology B: Biology, 209*, Article 111942.

Sheng, L., & Wang, L. (2021). The microbial safety of fish and fish products: Recent advances in understanding its significance, contamination sources, and control strategies. *Comprehensive Reviews in Food Science and Food Safety, 20*, 738–786.

Sheng, L., Zhang, Z., Sun, G., & Wang, L. (2020). Light-driven antimicrobial activities of vitamin K3 against *Listeria monocytogenes, Escherichia coli* O157:H7 and *Salmonella* Enteritidis. *Food Control, 114*, Article 107235.

Sheng, L., & Zhu, M.-J. (2021). Practical in-storage interventions to control foodborne pathogens on fresh produce. *Comprehensive Reviews in Food Science and Food Safety, 20*, 4584–4611.

Shih, M.-H., & Huang, F.-C. (2013). Repetitive methylene blue-mediated photoantimicrobial chemotherapy changes the susceptibility and expression of the outer membrane proteins of *Pseudomonas aeruginosa*. *Photodiagnosis and Photodynamic Therapy, 10*, 664–671.

Silva, A. F., Borges, A., Freitas, C. F., Hioka, N., Mikcha, J. M. G., & Simões, M. (2018). Antimicrobial photodynamic inactivation mediated by rose bengal and erythrosine is

effective in the control of food-related bacteria in planktonic and biofilm states. *Molecules, 23*, 2288.
Song, L., Zhang, F., Yu, J., Wei, C., Han, Q., & Meng, X. (2020). Antifungal effect and possible mechanism of curcumin mediated photodynamic technology against *Penicillium expansum*. *Postharvest Biology and Technology, 167*, Article 111234.
Subedi, S., Du, L., Prasad, A., Yadav, B., & Roopesh, M. S. (2020). Inactivation of *Salmonella* and quality changes in wheat flour after pulsed light-emitting diode (LED) treatments. *Food and Bioproducts Processing, 121*, 166–177.
Tan, Y., Cheng, Q., Yang, H., Li, H., Gong, N., Liu, D., Wu, J., & Lei, X. (2018). Effects of ALA-PDT on biofilm structure, virulence factor secretion, and QS in *Pseudomonas aeruginosa*. *Photodiagnosis and Photodynamic Therapy, 24*, 88–94.
Tao, R., Zhang, F., Tang, Q.-j., Xu, C.-s., Ni, Z.-J., & Meng, X.-h. (2019). Effects of curcumin-based photodynamic treatment on the storage quality of fresh-cut apples. *Food Chemistry, 274*, 415–421.
Wang, D., Kyere, E., & Ahmed Sadiq, F. (2021). New trends in photodynamic inactivation (PDI) combating biofilms in the food industry-A review. *Foods, 10*, 2587.
WHO. (2015). WHO estimates of the global burden of foodborne diseases: Foodborne diseases burden epidemiology reference group 2007-2015. https://www.who.int/publications/i/item/9789241565165. (Accessed 1 September 2021).
Willis, J. A., Cheburkanov, V., Kassab, G., Soares, J. M., Blanco, K. C., Bagnato, V. S., & Yakovlev, V. V. (2021). Photodynamic viral inactivation: Recent advances and potential applications. *Applied Physics Reviews, 8*, Article 021315.
Wu, J., Mou, H., Xue, C., Leung, A. W., Xu, C., & Tang, Q.-J. (2016). Photodynamic effect of curcumin on *Vibrio parahaemolyticus*. *Photodiagnosis and Photodynamic Therapy, 15*, 34–39.
Zhang, Z., Si, Y., & Sun, G. (2019). Photoactivities of vitamin K derivatives and potential applications as daylight-activated antimicrobial agents. *ACS Sustainable Chemistry & Engineering, 7*, 18493–18504.
Zhang, Q.-Z., Zhao, K.-Q., Wu, Y., Li, X.-H., Yang, C., Guo, L.-M., Liu, C.-H., Qu, D., & Zheng, C.-Q. (2017). 5-aminolevulinic acid-mediated photodynamic therapy and its strain-dependent combined effect with antibiotics on *Staphylococcus aureus* biofilm. *PLoS One, 12*, Article e0174627.
Zhu, S., Song, Y., Pei, J., Xue, F., Cui, X., Xiong, X., & Li, C. (2021). The application of photodynamic inactivation to microorganisms in food. *Food Chemistry X, 12*, 100150.